

SAMPLE-EFFICIENT ALIGNMENT FOR LLMs

Anonymous authors

Paper under double-blind review

ABSTRACT

We study methods for efficiently aligning large language models (LLMs) with human preferences given budgeted online feedback. We first formulate the LLM alignment problem in the frame of contextual dueling bandits. This formulation, subsuming recent paradigms such as online RLHF and online DPO, inherently quests for sample-efficient algorithms that incorporate *online active exploration*. Leveraging insights from bandit theory, we introduce a unified algorithm based on **Thompson sampling** and highlight its applications in two distinct LLM alignment scenarios. The practical agent that efficiently implements this algorithm, named **SEA** (Sample-Efficient Alignment), is empirically validated through extensive experiments across three model scales (1B, 2.8B, 6.9B) and three preference learning algorithms (DPO, IPO, SLiC). The results demonstrate that **SEA** achieves highly sample-efficient alignment with oracle’s preferences, outperforming recent active exploration methods for LLMs. We will release our codebase to hopefully accelerate future research in this field.

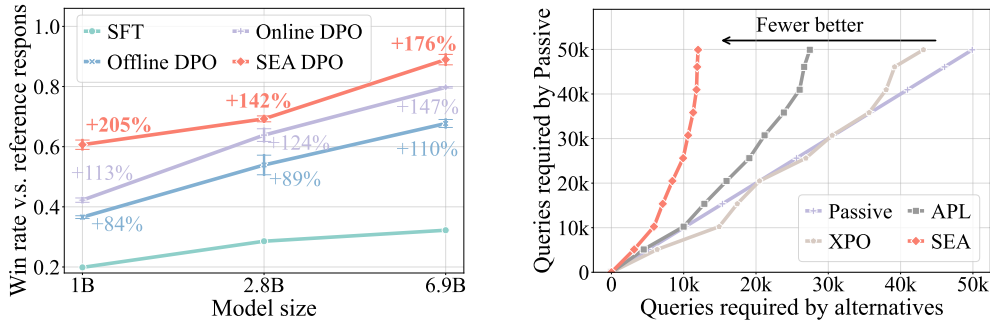


Figure 1: Win rate comparison of model responses against reference responses on the TL;DR task, judged by the preference oracle. All compared methods use the same optimization method (DPO). **(Left)** Performance improvements at convergence over SFT models achieved by offline (Offline DPO), passively online (Online DPO), and our *active exploration* (SEA DPO) methods. **(Right)** The number of queries required by the passively online method (Passive) versus that by different active exploration methods to attain various levels of win rates. SEA achieves the best sample efficiency for online alignment compared to XPO and APL.

1 INTRODUCTION

Aligning LLMs with human preferences is a crucial step to elicit various desirable behaviors, e.g., helpfulness and harmlessness (Bai et al., 2022). Moreover, it holds the potential to create superhuman capabilities with only human-level feedback, as verifying is believed to be easier than synthesizing novel behaviors. By iteratively generating massive new candidates and asking for human feedback, LLMs could learn to reinforce good behaviors and may eventually surpass human capabilities.

Existing methods, either via reinforcement learning from human feedback (RLHF) (Stiennon et al., 2020; Ouyang et al., 2022) or direct alignment from preferences (DAP) (Rafailov et al., 2023; Azar et al., 2024), typically require a large amount of human annotations to achieve effective alignment. As a result, the volume of human feedback becomes a major bottleneck in practical alignment scenarios. This poses a challenging and under-explored research question:

How to align LLMs sample-efficiently?

To seek answers, in Section 2, we formalize LLM alignment as a contextual dueling bandit (CDB) (Yue et al., 2012; Dudík et al., 2015), where the agent (i.e., the learner and decision maker, in

our case the LLM) interacts with the environment (i.e., human) to collect experience for improving its policy. This formulation naturally calls for two key properties for alignment algorithms to be sample-efficient:

Property 1 (Online interaction). Interacting and learning *online* allows the agent to act with the latest learned policy and then use that experience to immediately improve the policy.

Property 2 (Active exploration). An *actively exploring* agent strategically selects actions such that the collected experience leads to maximal policy improvement.

Since the CDB formulation is general and almost subsumes all existing LLM alignment methods, it provides us a lens to scrutinize prior methods on the axes of Properties 1 and 2. In Section 3, we thoroughly discuss prior alignment approaches, ranging from offline learning (Rafailov et al., 2023; Azar et al., 2024) and passive learning with iterative (Christiano et al., 2017; Dong et al., 2024) or online interaction (Guo et al., 2024), to active exploration for learning preference models (Dwaracherla et al., 2024) or aligning LLMs (Muldrew et al., 2024; Zhang et al., 2024a; Xie et al., 2024). As will be revealed, most prior methods (partially) fail to satisfy the two properties, resulting in inferior sample efficiency. Moreover, through the CDB formulation, we identify two LLM alignment scenarios, namely aligning from online users’ feedback (e.g., ChatGPT (2024)) and aligning from crowdsourcing (Christiano et al., 2017; Ouyang et al., 2022), and shed light on their correspondences to two bandit settings (explore & exploit and best arm identification). Understanding their differences is important for designing efficient alignment algorithms for respective scenarios. We detail these two settings in Section 2 and discuss how prior works approach them in Section 3.

Leveraging algorithmic insights from bandit theory, our answer to the research question above is a principled alignment algorithm based on Thompson sampling (TS) (Thompson, 1933). Our method fulfills Properties 1 and 2 to enhance sample efficiency, and it solves either of the two settings depending on practical scenarios (Section 4.1). We incorporate techniques including *epistemic reward model*, *policy-guided search* and *mixed preference learning* to implement the proposed TS algorithm (Section 4.2), yielding a practical agent which we call **SEA** (Sample-Efficient Alignment). In addition, we develop and open source a highly efficient, distributed learning system for studying online LLM alignment methods (Section 5), eliminating barriers to *fair* empirical comparisons of different alignment algorithms. Through extensive experiments (Section 6), **SEA** shows strong empirical results (see Figure 1), consistently achieving higher win rates and improved sample efficiency compared to baseline approaches across three model scales. We will open source the codebase to hopefully accelerate future research in this field.

2 LLM ALIGNMENT AS CONTEXTUAL DUELING BANDITS

We first review the definitions and two typical objectives of *Contextual Dueling Bandits* (Section 2.1), then translate them into the language of *LLM alignment* (Section 2.2). The tight connection between them, as we will see, allows us to leverage insights from bandit algorithms to design efficient alignment algorithms for LLMs.

2.1 CONTEXTUAL DUELING BANDITS

Contextual dueling bandits (CDB) (Yue et al., 2012; Dudík et al., 2015) is proposed to study online learning problems where the feedback consists of relative pairwise comparisons. A CDB problem can be characterized by a tuple $(\mathcal{C}, \mathcal{A}, \mathbb{P})$, where \mathcal{C} is the context space, \mathcal{A} is the action space, and $\mathbb{P} : \mathcal{A} \times \mathcal{A} \times \mathcal{C} \mapsto [0, 1]$ denotes the unknown *preference oracle*. An agent learns by iteratively interacting with the environment (i.e., the preference oracle \mathbb{P}) as follows. At each round t of the learning process, a context $c_t \sim p_{\mathcal{C}}$ is presented to the agent, who needs to take two actions $\mathbf{a}_t, \mathbf{a}'_t \in \mathcal{A}$ for a “dueling” comparison. The agent then receives stochastic feedback in the form of a **comparison result** $z_t \sim \text{Ber}(\mathbb{P}(\mathbf{a}_t \succ \mathbf{a}'_t | c_t))$ from the environment, where $\text{Ber}(\cdot)$ is the Bernoulli distribution and \succ denotes that the first action is preferred.

Regret. The quality of the dueling actions selected by the agent is measured by the *immediate regret*: $R_t = \mathbb{P}(\mathbf{a}_t^* \succ \mathbf{a}_t | c_t) + \mathbb{P}(\mathbf{a}'_t \succ \mathbf{a}'_t | c_t) - 1$, where \mathbf{a}_t^* is the best action¹ the agent would take at round t if it had complete knowledge of \mathbb{P} . Intuitively, if the agent has learned how to act optimally from round t onwards, it would no longer suffer any regret since its actions would be indistinguishable from the best action ($\mathbb{P}(\mathbf{a}_t^* \succ \mathbf{a}_t | c_t) = \frac{1}{2}$ hence $R_t = 0$ for $t \geq t$).

¹We assume that a best action \mathbf{a}^* in the sense that $\mathbb{P}(\mathbf{a}^* \succ \mathbf{a} | c) \geq \frac{1}{2}, \forall \mathbf{a} \in \mathcal{A}$ exists for all context $c \in \mathcal{C}$.

general:polished
these
two
para-
graphs

fdal

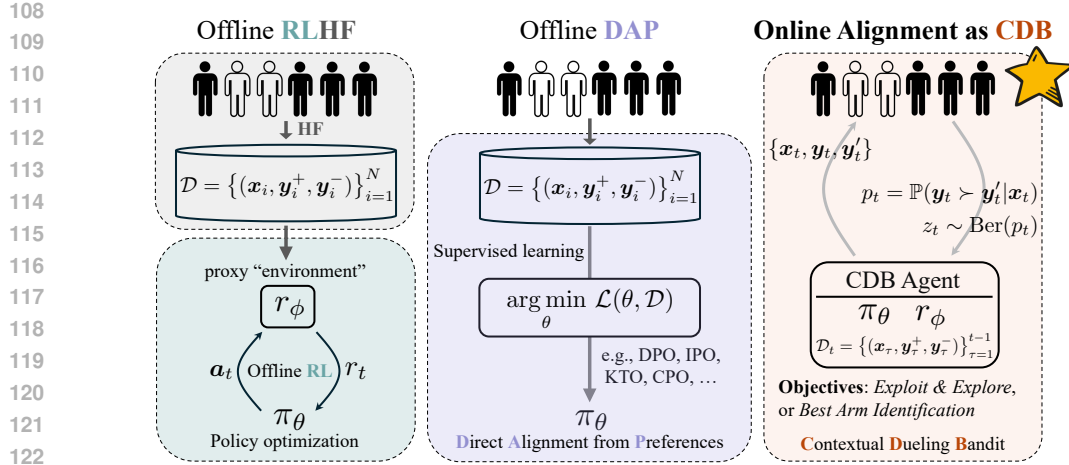


Figure 2: (Left) A typical offline RLHF pipeline consists of three stages: collecting preference dataset, training a reward model to serve as a proxy “environment”, and running RL to optimize the LLM policy inside the proxy “environment”. (Middle) DAP simplifies RLHF by merging the last two stages of RLHF into a single step of contrastive supervised learning. (Right) Unlike prior two offline approaches, online alignment employs a CDB interface, where the agent directly interacts with the preference oracle (e.g., humans) online, learning to produce *good* responses satisfying either E&E or BAI objectives. [general.fdaL: use fig.2 to provide a clearer comparison between our CDB formulation and RLHF/DPO.]

Optimal policy. A policy $\pi \in \Delta_{\mathcal{A}}^{\mathcal{C}}$ associates each context $c \in \mathcal{C}$ with a probability distribution $\pi(\cdot|c) \in \Delta_{\mathcal{A}}$ over the action space. The *total preference* of policy π over policy μ given a context sampling distribution $p_{\mathcal{C}} \in \Delta_{\mathcal{C}}$ and a preference oracle \mathbb{P} is defined as

$$P_{p_{\mathcal{C}}, \mathbb{P}}(\pi \succ \mu) = \mathbb{E}_{c \sim p_{\mathcal{C}}} [\mathbb{E}_{\mathbf{a} \sim \pi(\cdot|c)} \mathbb{E}_{\mathbf{a}' \sim \mu(\cdot|c)} [\mathbb{P}(\mathbf{a} \succ \mathbf{a}'|c)]] . \quad (1)$$

We adopt the *von Neumann winner* (Dudík et al., 2015) as the solution concept, which requires the optimal policy π^* to satisfy that

$$\forall \pi' \in \Delta_{\mathcal{A}}^{\mathcal{C}}, P_{p_{\mathcal{C}}, \mathbb{P}}(\pi^* \succ \pi') \geq \frac{1}{2} . \quad (2)$$

In words, the von Neumann winner policy should beat or tie with every policy (i.e., is zero-regret) on average.

Learning objectives. The goal of bandit agents is to learn an optimal policy through interactions with the environment. There are two subtypes of objectives that focus on different learning scenarios. The first type considers the conventional *explore and exploit (E&E)* setting (Robbins, 1952; Auer et al., 2002), where the agent learns fully **online** and tries to minimize the cumulative regret over T rounds: $\sum_{t=1}^T R_t$. The second type of objective concerns the *best arm identification (BAI)* setting (Bubeck et al., 2009; Audibert & Bubeck, 2010), where the agent is only evaluated **offline** on its average performance, possibly at any round (a.k.a., anytime regret), and tries to learn the optimal policy with minimum interaction. Both settings call for effective *online exploration* strategies that satisfy Properties 1 and 2. Their differences will be made clearer with real scenarios in Section 2.2.

2.2 ONLINE ALIGNMENT AS CDB

Online LLM alignment can be framed as a CDB problem as illustrated in Figure 2 (Right). Specifically, at time t a text prompt (cf. context) $x_t \in \mathcal{X}$ is sampled from a prompt distribution $p_{\mathcal{X}}$. Then, two distinct responses (cf. actions), $y_t, y'_t \in \mathcal{Y}$, are chosen by the agent, and presented to human annotators (cf. the environment) for preference ranking. The winning and losing responses are labeled as (y_t^+, y_t^-) based on a binary stochastic feedback $z_t \sim \text{Ber}(\mathbb{P}(y_t \succ y'_t|x_t))$. The agent is expected to produce *good* responses satisfying either E&E or BAI objectives, with knowledge learned from the experience accumulated so far: $\mathcal{D}_t = \{(x_{\tau}, y_{\tau}^+, y_{\tau}^-)\}_{\tau=1}^t$. A standard assumption is that human preferences follow the Bradley-Terry (BT) model (Bradley & Terry, 1952):

$$\mathbb{P}(y_t \succ y'_t|x_t) = \frac{\exp(r^*(x_t, y_t))}{\exp(r^*(x_t, y_t)) + \exp(r^*(x_t, y'_t))} = \sigma(r^*(x_t, y_t) - r^*(x_t, y'_t)), \quad (3)$$

²We denote by $\Delta_{\mathcal{A}}^{\mathcal{C}}$ the set of all mappings $\mathcal{C} \mapsto \Delta_{\mathcal{A}}$, where $\Delta_{\mathcal{A}}$ denotes the set of all probability distributions over \mathcal{A} .

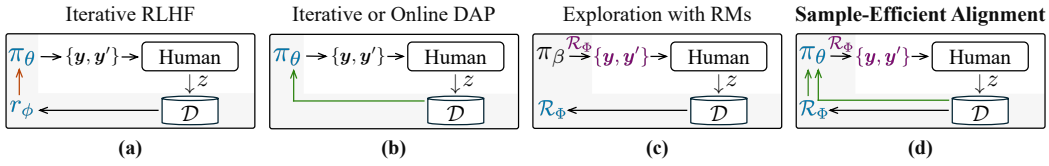


Figure 3: Different paradigms to solve online LLM alignment in the CDB interface (Figure 2 (Right)). The CDB agent is shaded in gray. We use colors to denote **learnable components**, **RL optimizer**, **direct optimizer**, and **active exploration**. r_ϕ denotes a point estimate of human’s implicit reward, while \mathcal{R}_ϕ refers to an uncertainty-aware reward model. Please see Section 3 for detailed comparisons with references to prior works. [fdaL: updated fig.3 to highlight the differences between (b) and (d).]

where σ is the sigmoid function and r^* encodes human’s implicit reward. The immediate regret of LLM alignment can be rewritten as $R_t = r^*(\mathbf{x}_t, \mathbf{y}_t^*) - (r^*(\mathbf{x}_t, \mathbf{y}_t) + r^*(\mathbf{x}_t, \mathbf{y}_t'))/2$ with the BT assumption (Saha, 2021; Li et al., 2024), where \mathbf{y}_t^* is the best response for prompt \mathbf{x}_t given human’s implicit reward, i.e., $r^*(\mathbf{x}_t, \mathbf{y}_t^*) \geq r^*(\mathbf{x}_t, \mathbf{y}), \forall \mathbf{y} \in \mathcal{Y}$. The von Neumann winner policy is also redefined as

$$\pi^* \in \arg \max_{\pi \in \Delta_{\mathcal{Y}}} J(\pi), \text{ where } J(\pi) = \mathbb{E}_{\mathbf{x} \sim p_{\mathcal{X}}} \mathbb{E}_{\mathbf{y} \sim \pi(\cdot|\mathbf{x})} [r^*(\mathbf{x}, \mathbf{y})] \text{ is the objective,} \quad (4)$$

by substituting Eq. (3) into Eq. (1) and maximizing $P_{p_{\mathcal{X}}, \mathbb{P}}(\pi \succ \pi^*)$ towards $1/2$.

The **two settings in bandits** have their respective applications in LLM alignment. **(1)** The E&E setting applies to the scenario of serving an LLM-based application online and aligning it continually with users’ preferences. In this setting, the agent needs to balance exploration with exploitation, thus the cumulative regret is of interest because the quality of *every* response matters. In fact, commercial systems like ChatGPT would strategically ask users to make a dueling comparison, while upholding the quality of both responses. Please see Figure 12 in Appendix G for an example. **(2)** The BAI setting corresponds to the other scenario where annotators are paid to provide human feedback (Christiano et al., 2017; Ouyang et al., 2022). The desideratum in this scenario is to align the LLM at the minimum labeling cost, while the quality of the dueling responses is not important as long as the experience helps sample-efficiently learn the von Neumann winner policy.

After formalizing LLM alignment in the framework of CDB and uncovering their tight connections, we next thoroughly discuss existing alignment methods in the CDB framework and reveal the sources of their sample inefficiencies.

3 HOW PRIOR WORKS (PARTIALLY) SOLVE LLM ALIGNMENT AS CDB

We first align the notations and terminology used in CDB with commonly referred ones in the LLM community. Previously, we used the term “agent” to denote the learner and decision maker, and referred to its overall behavior as the “policy” π (as in Eq. (4)), following the standard abstraction in RL (Sutton & Barto, 2018; Sutton et al., 2022). However, in the LLM literature, “policy” typically refers to the generative language model alone, excluding components like reward models (RMs) that the agent might additionally build (see Figure 2 (Right)). To avoid confusion, from now on we use π_{θ^t} to denote the generative language model (policy) and r_{ϕ^t} to denote the (optional) RM at time t , both of which are learned from preference data \mathcal{D}_t collected up to time t . We will omit t when the time-indexing is not applicable (i.e., no online interaction) or not important in the context.

RLHF and DAP. Commonly adopted RLHF pipelines (Christiano et al., 2017; Stiennon et al., 2020; Bai et al., 2022; Ouyang et al., 2022) first learn a proxy RM with a negative log-likelihood loss:

$$\mathcal{L}_r(\phi|\mathcal{D}) = -\mathbb{E}_{(\mathbf{x}, \mathbf{y}^+, \mathbf{y}^-) \sim p_{\mathcal{D}}} [\log \sigma(r_\phi(\mathbf{x}, \mathbf{y}^+) - r_\phi(\mathbf{x}, \mathbf{y}^-))], \quad (5)$$

where \mathcal{D} is collected by querying human annotators using a behavior policy π_{ref} (typically the supervised fine-tuned policy π_{sft}). Afterwards, **offline RL**³ (Lange et al., 2012; Levine et al., 2020) is conducted to learn π_θ with respect to the learned reward r_ϕ **internally** within the agent (Figure 3a). However, the learned model π_θ might be inaccurate at regions out of the distribution (o.o.d.) of π_{ref} because little training data can be collected. An effective remedy is to incorporate a pessimistic term to combat the distributional shift, leading to a reformulation of the von Neumann winner

³Offline in the sense that π_θ is not directly learned from online human feedback. See Appendix B for details.

general:polished
sec.3

RtS4

fdaL

policy objective in Eq. (4) as

$$J(\pi_\theta) = \mathbb{E}_{\mathbf{x} \sim p_{\mathcal{X}}} \mathbb{E}_{\mathbf{y} \sim \pi_\theta(\cdot|\mathbf{x})} \left[\underbrace{r_\phi(\mathbf{x}, \mathbf{y})}_{\text{estimated } r^*} - \beta \log \frac{\pi_\theta(\mathbf{y}|\mathbf{x})}{\pi_{\text{ref}}(\mathbf{y}|\mathbf{x})} \right] \quad (6)$$

$$= \mathbb{E}_{\mathbf{x} \sim p_{\mathcal{X}}} \left[\mathbb{E}_{\mathbf{y} \sim \pi_\theta(\cdot|\mathbf{x})} [r_\phi(\mathbf{x}, \mathbf{y})] - \beta D_{\text{KL}}(\pi_\theta(\cdot|\mathbf{x}) || \pi_{\text{ref}}(\cdot|\mathbf{x})) \right], \quad (7)$$

which converts an online objective regarding the human’s implicit reward r^* to an offline objective regarding the proxy reward r_ϕ . The KL penalty in Eq. (7) is widely used for language model fine-tuning (Jaques et al., 2020; Xiong et al., 2024), and PPO (Schulman et al., 2017) has become a default *RL optimizer* to maximize the KL-regularized reward. However, the performance of RLHF is guaranteed only if the preference data \mathcal{D} induced by π_{ref} adequately covers π^* (Zhu et al., 2023), which is often approximated by updating π_{ref} with the latest (improved) π_θ for re-sampling a batch of online experience and repeating Eq. (5) and (7). Prior works typically focus on offline (Figure 2 (Left)) or iterative online (with only a few iterations) settings (Xiong et al., 2024; Dong et al., 2024), which may compromise sample efficiency (Property 1).

True online RLHF is difficult due to the complexity and instability of RL optimizers. For example, Huang et al. (2024) openly reproduces offline RLHF scaling behaviors but requires many implementation tricks for training, highlighting the difficulties of an online counterpart. Fortunately, the introduction of DAP (or *direct optimizers*) largely simplifies and stabilizes fine-tuning by conducting contrastive supervised learning directly on \mathcal{D} (Figure 3b). While most DAP works focus on learning from a fixed offline preference dataset (Figure 2 (Middle), including Zhao et al. (2023); Rafailov et al. (2023); Azar et al. (2024); Meng et al. (2024); Zhang et al. (2024b)), iterative DPO (Xu et al., 2023) observes improved results when allowing iterative online interaction. Guo et al. (2024) further propose OAIF to make DAP faithfully online, satisfying Property 1, and demonstrate that online learning prevents over-fitting and yields continual performance improvement. Nevertheless, it still employs passive exploration strategies (using $\mathbf{y}, \mathbf{y}' \sim \pi_\theta$), hindering sample efficiency (Property 2).

Online exploration in LLMs. A line of recent works (Mehta et al., 2023; Das et al., 2024; Melo et al., 2024; Dwaracherla et al., 2024) adopts the fully online bandit formulation and incorporates *active exploration* with uncertainty-aware RMs for response selection (Figure 3c). In particular, Mehta et al. (2023) consider the E&E setting and develop a UCB-style (Auer et al., 2002) algorithm; Das et al. (2024) instead select the dueling responses with the most uncertain preference estimate, targeting the BAI setting in a pure exploration way; unlike the above, Melo et al. (2024) view the problem from the angle of pool-based active learning and propose an acquisition function based on both entropy and epistemic uncertainty; finally, the work by Dwaracherla et al. (2024) is the closest to ours in the sense that they apply double Thompson sampling (DTS) (Wu & Liu, 2016) for exploration, but DTS is designed for the E&E setting while they evaluate anytime average performance as in the BAI setting. We will show in Appendix E.1 that pure exploration by Das et al. (2024) is not the best choice for BAI, and the objective mismatch in Dwaracherla et al. (2024) could lead to sub-optimal performance in respective settings. Meanwhile, all these works primarily focus on learning uncertainty-aware RMs online without updating LLM policies. Therefore, all responses are sampled from a fixed proposal policy π_β (or even a fixed dataset), making the data coverage a critical concern.

Another line of research updates LLMs online while incorporating exploration. Zhang et al. (2024a) and Xie et al. (2024) independently propose to learn an optimistic RM to encourage exploration. They leverage the property of DPO (Rafailov et al., 2023) to reparameterize RM with policy and conclude with an extra optimistic term in the DPO loss function. Thus, their learning processes are like Figure 3b but with an optimistic direct optimizer. Muldrew et al. (2024) adopt the vanilla DPO loss but utilize the implicit reward margin to actively select dueling responses. Yet, these methods are tightly coupled with DPO and not compatible to other direct optimizers. Their experiments are also limited to a few online iterations, possibly due to the implementation difficulty of a faithfully online learning system. Given their relevance to our approach, we will reproduce them in a fully online manner for fair comparisons in Section 6.1. We summarize prior works in Table 3 in Appendix G.

4 SEA: SAMPLE-EFFICIENT ALIGNMENT FOR LLMs

In this section we present our online exploration agent SEA (Figure 3d). We first introduce a principled Thompson sampling algorithm inspired by bandit theory (Section 4.1), and then derive SEA as

Algorithm 1 Thompson sampling for LLM alignment (intractable).

Input: Prompt distribution $p_{\mathcal{X}}$, unknown but queryable preference oracle \mathbb{P} .

- 1: Initialize experience $\mathcal{D}_0 \leftarrow \emptyset$.
- 2: **for** $t = 1, \dots, T$ **do**
- 3: Receive a prompt $\mathbf{x}_t \sim p_{\mathcal{X}}$.
- 4: Sample $r \sim p_r(\cdot|\mathcal{D}_{t-1})$ and set $\mathbf{y}_t \leftarrow \arg \max_{\mathbf{b} \in \mathcal{Y}} r(\mathbf{x}_t, \mathbf{b})$. // Select 1st response \mathbf{y} .
- 5: **repeat**
- 6: Sample $r \sim p_r(\cdot|\mathcal{D}_{t-1})$ and set $\mathbf{y}'_t \leftarrow \arg \max_{\mathbf{b} \in \mathcal{Y}} r(\mathbf{x}_t, \mathbf{b})$. // Select 2nd response \mathbf{y}' .
- 7: **until** $\mathbf{y}'_t \neq \mathbf{y}_t$
- 8: **BAI objective: labeling via crowdsourcing.**
- 9: Set $\mathbf{y}'_t \leftarrow \arg \max_{\mathbf{b} \in \mathcal{Y}} \mathbb{V}[\sigma(r(\mathbf{x}_t, \mathbf{y}_t) - r(\mathbf{x}_t, \mathbf{b}))]$, // OR select 2nd response \mathbf{y}' .
- 10: where $\mathbb{V}[\cdot]$ computes variance over the posterior $p_r(\cdot|\mathcal{D}_{t-1})$.
- 11: Query \mathbb{P} to label $\{\mathbf{y}_t, \mathbf{y}'_t\}$, and update experience $\mathcal{D}_t \leftarrow \mathcal{D}_{t-1} \cup \{(\mathbf{x}_t, \mathbf{y}_t^+, \mathbf{y}_t^-)\}$.
- 12: **end for**

// See Algorithm 2 for a practical version.

its practically efficient implementation (Section 4.2). Interestingly, **SEA** can also be viewed as an instantiation of a classical model-based RL architecture called Dyna (Sutton, 1990), for which we defer the discussion to Appendix B.

4.1 THOMPSON SAMPLING FOR LLM ALIGNMENT

Thompson sampling (TS) (Thompson, 1933) is widely adopted for solving bandit problems at scale due to its efficiency and strong empirical performance in general online learning problems (Chapelle & Li, 2011; Russo et al., 2018). A bandit agent using Thompson sampling typically maintains and incrementally updates a posterior distribution of the oracle reward $p(r|\mathcal{D})$. Meanwhile, the agent takes actions following a greedy policy with respect to a sampled RM: $\mathbf{a}_t = \arg \max_{\mathbf{a}} r(\mathbf{a})$ with $r \sim p_r(\cdot|\mathcal{D})$. This simple yet effective algorithm naturally balances exploration and exploitation: when the agent has limited knowledge about the environment, the posterior estimate exhibits high uncertainty so that the sampled RM could guide the greedy policy to explore; after sufficient experience is gathered, the sampled RM approximates the oracle more closely, allowing the agent to exploit near-optimal policies.

In the context of LLM alignment, we leverage the BT assumption (Eq. (3)) to replace the preference oracle \mathbb{P} with human’s implicit reward r^* . This substitution enables us to model the reward posterior $p(r|\mathcal{D})$ in the standard TS framework, preserving the probabilistic structure necessary for effective posterior sampling. Inspired by prior works (Wu & Liu, 2016; González et al., 2017) on non-contextual K -arm bandits and preferential Bayesian optimization problems, we generalize them for LLM alignment and develop a unified algorithm as shown in Algorithm 1. Note that we assume for now the LLM agent can be fully described by the posterior $p(r|\mathcal{D})$, and we defer practical reward (r_ϕ) and policy (π_θ) learning to Section 4.2.

As Algorithm 1 presents, the first response of the duel is always selected via standard TS (Line 4). The selection of the second response varies across different settings. Line 5 will be used for scenarios where preference feedback is collected from online users (the E&E setting). The dueling responses selected in this case will both try to maximize a sampled RM, so that the online user experience is warranted with best effort. However, such algorithm can have poor asymptotic performance for BAI problems (Russo, 2016), because sub-optimal responses with confidently high rewards might be tried for a long time at the expense of not exploring other potentially better choices. In light of this, Line 6 provides an alternative for scenarios where we could hire annotators for feedback and low-quality but exploratory responses are safe to try. Specifically, Line 6 selects the second response as the one that maximizes the variance of the preference (Eq. (3)) over the first response \mathbf{y}_t . This variance quantifies the *epistemic uncertainty* of the RM, pointing the agent to the maximally informative direction to explore for better sample efficiency.

However, Algorithm 1 is yet to be practical for LLM alignment for three main reasons. First, computing and sampling from a reward posterior is intractable for nearly all RMs at LLM scale, which are mostly based on large transformers (Lambert et al., 2024). Second, even if we managed to approximate the reward posterior, the **arg max** operations for response selection are still intractable

since the search space \mathcal{Y} is discrete and massive for token sequences of arbitrary length. Last but not least, an LLM agent (Achiam et al., 2023; Touvron et al., 2023) typically consists in a generative model π_θ (e.g., a transformer (Vaswani et al., 2017)), while the algorithm above is centered around a reward posterior $p(r|\mathcal{D})$ that cannot be easily converted into a generative model. We next detail how SEA practically addresses the three aforementioned issues.

4.2 PRACTICAL IMPLEMENTATION

4.2.1 EPISTEMIC REWARD MODEL FOR POSTERIOR SAMPLING

To implement active exploration with TS, we seek an efficient way to maintain and incrementally update the reward posterior $p(r|\mathcal{D})$. We consider *deep ensemble* for our purpose, due to its capability to model epistemic uncertainty (Lakshminarayanan et al., 2017) and provable results when applied to TS in linear bandits (Qin et al., 2022). Specifically, we update a set of plausible RMs independently and online, using the preference data and a regularized negative log-likelihood loss:

$$\mathcal{L}_{\mathcal{R}}(\Phi^t|\mathcal{D}_t) = \sum_{k=1}^K (\mathcal{L}_r(\phi_k^t|\mathcal{D}_t) - \lambda \|\phi_k^t - \phi_k^0\|), \quad (8)$$

where \mathcal{L}_r is defined in Eq. (5), $\Phi^t = \{\phi_k^t\}_{k=1}^K$ contains the weights of the ensemble of size K , and λ controls the regularization towards individual initial weights ϕ_k^0 . **Each ensemble member is initialized independently with random weights, and then trained with regularization to maintain the diversity across ensemble members (Dwaracherla et al., 2024). Randomly picking a ϕ_k^t from Φ^t would approximate the posterior sampling ($r \sim p_r(\cdot|\mathcal{D}_t)$) for the RM (Lu & Van Roy, 2017; Gustafsson et al., 2020).** In practice, we train K MLP heads on top of a pretrained and frozen transformer. We refer to the ensemble as the Epistemic Reward Model (ERM, denoted as \mathcal{R}_Φ).

4.2.2 POLICY-GUIDED SEARCH TO APPROXIMATE $\arg \max$

With the ERM approximating the reward posterior, we need to further approximate the response selection steps (Lines 4 to 6) which generally take the form of $\arg \max_{\mathbf{b} \in \mathcal{Y}} U(\mathbf{b})$, where U absorbs the sampled prompt, the sampled RM, and optionally the selected first response (for BAI, Line 6). To obtain the maximum, bandit algorithms for large action spaces typically resort to an action optimization oracle (Katz-Samuels et al., 2020; Zhu et al., 2022), but they assume a linear structure of U with respect to \mathbf{b} , which might be impractical for LLMs. Therefore, we instead replace the optimization over \mathcal{Y} with sampling from a policy-guided distribution conditioned on U , $\pi_{\text{prior}}(\cdot|\mathbf{x}) \exp(U(\cdot)/\eta)$, which is appropriate since it favors responses \mathbf{y} that approximately maximize $U(\mathbf{y})$. In practice, for a given prompt \mathbf{x}_t , we sample M candidate responses from the prior policy $\pi_{\text{prior}}(\cdot|\mathbf{x}_t)$ to construct a proposal set $\mathcal{S}_t = \{\mathbf{y}_t^i\}_{i=1}^M$. We then conduct a greedy search in \mathcal{S}_t (taking $\eta \rightarrow 0$) to identify the response \mathbf{y}_t (or \mathbf{y}_t^i) that locally maximizes the utility function U , which is subsequently used in the duel. We also reuse the same \mathcal{S}_t for different U functions at time t to save computation. The choice of π_{prior} will be discussed in the next section.

4.2.3 ONLINE POLICY LEARNING FROM MIXED PREFERENCES

We finally resolve two remaining questions: (Q1) how to choose a sensible π_{prior} at each time t and (Q2) how to get a good generative policy online. To this end, we propose a simple approach to approximately address both questions simultaneously. That is, we can utilize any direct optimizer to learn the policy π_{θ^t} online with the following loss and use the latest online policy as π_{prior} :

$$\mathcal{L}_\pi(\theta^t|\mathcal{B}_t, \pi_{\text{ref}}, F) = \mathbb{E}_{(\mathbf{x}, \mathbf{y}^+, \mathbf{y}^-) \sim p_{\mathcal{B}_t}} [F_{\theta^t}(\mathbf{x}, \mathbf{y}^+, \mathbf{y}^-, \pi_{\text{ref}})], \quad (9)$$

where \mathcal{B}_t is a batch of preference data labeled by the oracle wherein the responses are proposed by π_{prior} and selected by \mathcal{R}_{Φ^t} , F could be any DAP loss (see Appendix A for some examples), and π_{ref} is chosen to be π_{sft} . Note that we use π_{θ^t} as π_{prior} at any time t , thus \mathcal{B}^t is a batch of on-policy data. By *contrastive training* on these *on-policy* data, we leverage their orthogonal benefits to achieve maximal policy improvement (Tajwar et al., 2024; Tang et al., 2024).

Now that optimizing Eq. (9) yields a good online policy π_{θ^t} (answering Q2), we need to assess whether π_{θ^t} can serve as a suitable π_{prior} for approximating the $\arg \max$ in TS (Q1). If we optimize π_{θ^t} with oracle preference data, \mathcal{S}_t will be biased towards responses with high oracle reward r^* . Bias towards high- r^* region is generally helpful because it aligns with $\arg \max_{\mathbf{b} \in \mathcal{Y}} r(\mathbf{x}, \mathbf{b})$ that seeks high-reward responses. However, optimizing π_{θ^t} *only* with oracle data can average out the

epistemic uncertainty of \mathcal{R} , hindering the exploration efficiency. To mitigate this issue, we further align π_{θ^t} with \mathcal{R}_{Φ^t} using the same direct optimizer to encourage π_{θ^t} to propose high- $r_{\phi_k^t}$ responses for individual $r_{\phi_k^t}$, leading to better approximation of $\arg \max_{\mathbf{b} \in \mathcal{Y}} r(\mathbf{x}, \mathbf{b})$ for any sampled r . To implement, we optimize Eq. (9) over a mixture distribution $p_{\mathcal{B}_t^{\text{mix}}} = \gamma p_{\mathcal{B}_t} + (1 - \gamma) p_{\mathcal{B}_t^{\text{ERM}}}$, where $\gamma \in [0, 1]$ controls the mixture ratio and $\mathcal{B}_t^{\text{ERM}} = \{(\mathbf{x}_i, \tilde{\mathbf{y}}_i^+, \tilde{\mathbf{y}}_i^-)\}_{i=1}^b$ consists of preference data labeled by randomly sampled individual ensemble members $r_{\phi_k^t}$. Interestingly, learning from mixed preferences further boosts sample efficiency because it utilizes the internal ERM to get pseudo labels instead of querying humans. This relates closely to model-based RL, for which we discuss further in Appendix B. We summarize our practical algorithm (Algorithm 2) in Appendix A.

5 EXPERIMENTAL SETUP

In this section, we elaborate the experimental setup employed to validate our algorithm and ensure fair comparisons with other online alignment baselines. We start by introducing the distributed learning system designed for experimenting with online LLM alignment using simulated human preferences (Section 5.1). Then, we provide key experimental details in Section 5.2, with a full description available in Appendix D.

5.1 DISTRIBUTED LEARNING SYSTEM

The interactive nature of LLM alignment necessitates an integrated online learning system that simulates the interface depicted on the right of Figure 2. The absence of a performant open-source online alignment system has restricted many existing works to only a few iterations of batch learning (Muldrew et al., 2024; Dong et al., 2024; Chen et al., 2024; Zhang et al., 2024a; Xie et al., 2024), which creates a mismatch with their theories that typically require a large number of online interaction rounds. Even worse, such absence also makes the comparison between different LLM exploration methods difficult, often restricting evaluations to the simplest iterative DAP baselines (Zhang et al., 2024a; Xie et al., 2024).

To fill this gap, we build a highly efficient learning system for experimenting with online LLM alignment algorithms. We notice that the computational bottleneck lies in online response sampling (i.e., autoregressive generation) and preference labeling (e.g., human, large RMs, or large LLMs), which mirrors the slow actor-environment interaction seen in RL systems. Inspired by distributed deep RL systems which spawn many actors or environments in parallel (Espoholt et al., 2018; Weng et al., 2022), we design an Actor-Learner-Oracle architecture for online LLM alignment, which is depicted in Figure 4. The three types of workloads (i.e., actor, learner and oracle) are heterogeneous and require different optimization. In particular, we adopt vLLM (Kwon et al., 2023) for the actor to accelerate the autoregressive response generation. We also use DeepSpeed’s ZeRO (Rasley et al., 2020; Rajbhandari et al., 2020) strategies to enhance the memory efficiency of the learner. The updated model weights are broadcasted from the learner master to all actors after every optimizer step efficiently via NCCL, similar to Hu et al. (2024). Furthermore, to improve the scalability, we wrap the oracle RM as a service using Mosec (Yang et al., 2021b), which supports dynamic batching and parallel processing, to minimize preference query latency. Finally, we leverage DeepMind Launchpad (Yang et al., 2021a) to compose all workloads into a distributed program and adopt Plasma (Philipp & Robert, 2017) to efficiently transfer data across process boundaries.

We benchmark our system’s efficiency against a concurrent implementation of online DPO by HuggingFace⁴, which utilizes only DeepSpeed for memory optimization. Our system achieves up to $2.5\times$ latency reduction compared to this counterpart, demonstrating its computational efficiency. Due to space constraints, detailed benchmarking methods and results are presented in Appendix F.

5.2 SETTINGS

We adopt SFT models tuned on TL;DR (Stiennon et al., 2020) from Huang et al. (2024), which cover three scales (1B, 2.8B, 6.9B) of the Pythia family (Biderman et al., 2023), as starting points

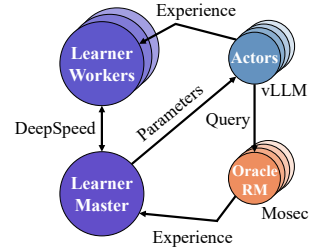


Figure 4: The learning system for experimenting online LLM alignment algorithms.

⁴https://huggingface.co/docs/trl/main/en/online_dpo_trainer.

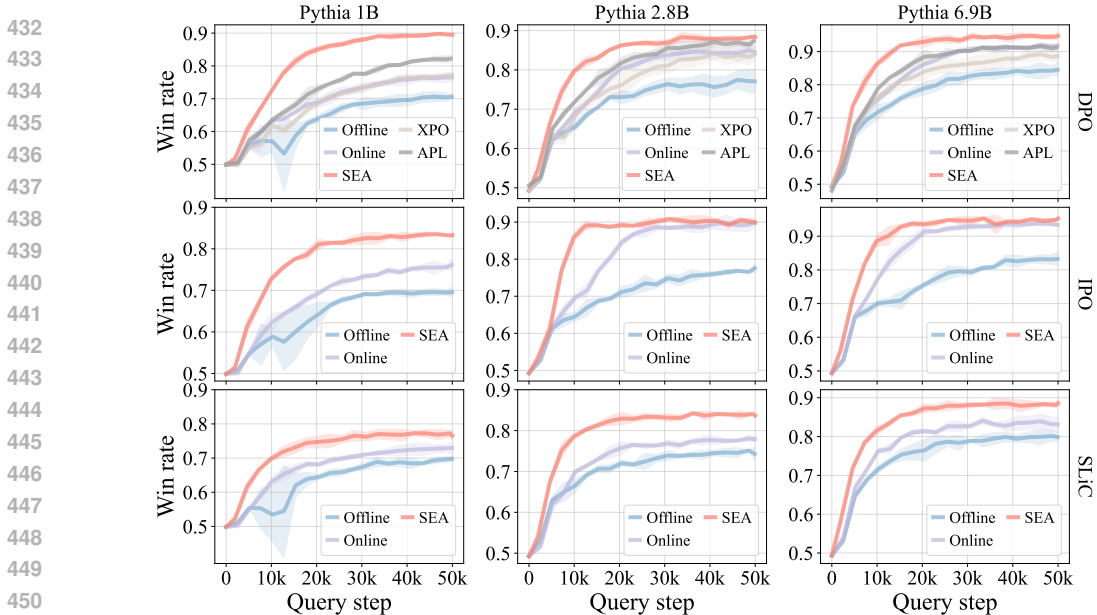


Figure 5: Win rate comparison of different algorithms against their initial SFT models across three scales and three direct optimizers.

for our experiments. We use a strong scalar RM (Liu et al., 2024a)⁵ to simulate the preference oracle. To verify the effectiveness of **SEA**, we employ three direct optimizers: DPO (Rafailov et al., 2023), IPO (Azar et al., 2024), and SLiC (Zhao et al., 2023) to serve as F in Eq. (9). Besides, two LLM exploration methods built on DPO, APL (Muldrew et al., 2024) and XPO (Xie et al., 2024), are fairly compared when using DPO as the optimizer. Our experiments primarily focus on the BAI setting (crowdsourcing labeling), where we report the win rate of learned models against initial SFT models. **All experiments are repeated three times to ensure statistical significance.** Please see Appendix D for more details.

6 EMPIRICAL STUDIES

We next present our empirical studies highlighting four results: **(1)** Comparisons with baselines across various direct optimizers and model scales demonstrate **SEA**’s superior *sample efficiency* (Section 6.1). **(2)** Ablations confirm that both *online policy learning* and *active exploration* contribute to sample-efficient alignment, and using the learned ERM for Best-of-N sampling further improves the performance (Section 6.2). **(3)** Different exploration strategies (Line 5 or Line 6 in Algorithm 1) are verified to work best in respective settings. **(4)** **SEA** robustly outperforms baselines when GPT4o-mini is used as a judge to simulate human feedback. **Results for (3-4) are deferred to Appendices E.1 and E.2 due to space constraints.**

6.1 OVERALL COMPARISON

We first compare **SEA** with all baselines across three model scales and three direct optimizers. APL and XPO are only compared when DPO is used as the direct optimizer, because they are incompatible with IPO or SLiC. Figure 5 shows the win rate curves versus the number of query steps. Across all settings, Online agents consistently improve sample efficiency over their Offline counterparts, validating the necessity of Property 1 for alignment algorithms. Focusing on the first row, we observe that among prior active exploration methods, XPO gives a small improvement in final performance over Online (passive) at the 1B scale, but falls short for larger scales. On the other hand, APL shows a significant sample efficiency boost at the 1B scale, but this advantage diminishes when scaling up and it performs almost the same as Online at 6.9B scale. Our method, **SEA**, outperforms both offline and online passive methods across all scales and all direct optimizers, confirming the critical role that Property 2 plays for sample-efficient alignment. Meanwhile, in the special case of using DPO as the direct optimizer, **SEA** also shows superior performance to prior online active exploration methods including APL and XPO. We invite readers to revisit Figure 1,

⁵<https://huggingface.co/Skywork/Skywork-Reward-Llama-3.1-8B>.

Table 1: Decomposition of different driving factors of online active alignment algorithms.

Variant	Inference (Test)	Exploration	Learn	Remark
1	π_θ	passive	π_θ	Online DAP (Guo et al., 2024)
2	π_θ	active	$(\pi_\theta, \mathcal{R}_\Phi)$	SEA without ERM sync (Section 4.2.3)
3	π_θ	active	$(\pi_\theta \leftrightarrow \mathcal{R}_\Phi)$	SEA
4	$\text{BoN}(\pi_\theta, \mathcal{R}_\Phi)$	passive	$(\pi_\theta, \mathcal{R}_\Phi)$	-
5	$\text{BoN}(\pi_\theta, \mathcal{R}_\Phi)$	active	$(\pi_\theta, \mathcal{R}_\Phi)$	-
6	$\text{BoN}(\pi_\theta, \mathcal{R}_\Phi)$	active	$(\pi_\theta \leftrightarrow \mathcal{R}_\Phi)$	SEA with Best-of-N sampling
7	$\text{BoN}(\pi_{\text{ref}}, \mathcal{R}_\Phi)$	active	\mathcal{R}_Φ	Not learn policy (Dwaracherla et al., 2024)

where we show that **SEA** not only attains significantly improved final performance (Left) but also achieves 2-5 \times better sample efficiency (Right).

Additionally, we note that the choice of direct optimizer matters for both online learning and active exploration. When comparing different optimizers at 1B scale (the first column), all Offline agents demonstrate comparable learning efficiency and reach the same level of final performance (around 70% win rate), but SLiC Online agent deliver slightly less improvement than DPO and IPO Online agents. Besides, when incorporating active exploration, the **SEA** agent using DPO shows much larger improvement than the other two. This suggests that selecting the most suitable policy optimizer coupled with active exploration would yield the best agent.

6.2 ABLATION ANALYSIS

Next, we decompose **SEA** into distinct components to evaluate their individual contributions. Table 1 shows the three axes we dissect **SEA** on, including inference methods, exploration strategies, and learning components. We construct seven agent variants from different combinations, which cover two closely related baselines (Guo et al., 2024; Dwaracherla et al., 2024). We show in Figure 6 the performance curves of each variant, all trained with DPO on 1B scale.

The left plot compares variants that directly use the policy for inference. It clearly shows the benefits of learning ERM for active exploration (Variant-2) and aligning π_{θ^t} with \mathcal{R}_{Φ^t} (Variant-3). Since a reward model is learned within the agent, we can further incorporate inference-time alignment via Best-of-N (BoN) sampling (Nakano et al., 2021; Touvron et al., 2023). This also facilitates a direct comparison between **SEA** and Dwaracherla et al. (2024), which learns a similar ERM for both exploration and BoN but does not align the LLM policy. Results in the right plot of Figure 6 suggest a similar trend that Variant-6 \succ Variant-5 \succ Variant-4. The Variant-7 (Dwaracherla et al., 2024), however, ceases to improve after ERM converges due to the limited capability of its fixed policy.

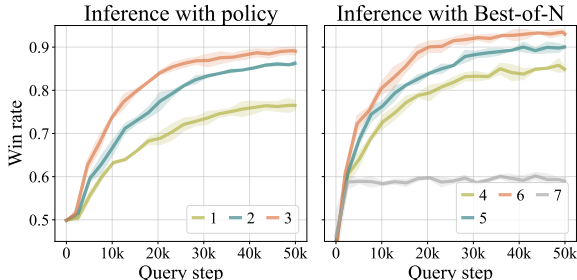


Figure 6: Win rate comparison of different agent variants when using (Left) policy and (Right) Best-of-N sampling for inference.

7 CONCLUSION

In this paper, we study the problem of LLM alignment through the lens of contextual dueling bandits and propose a Thompson sampling-based algorithm to achieve sample-efficient alignment. We incorporate three techniques, including epistemic reward model, policy-guided search and mixed preference learning to yield a practically efficient online alignment method. Extensive empirical evaluation demonstrates the superior sample efficiency of our method compared to existing baselines. To our knowledge, this is the first work to study active exploration for online LLM alignment with fully online experimental verification. We hope our positive empirical results, along with the open-sourced codebase, will encourage future research in this direction, ultimately enabling LLMs to achieve superhuman intelligence with an affordable amount of human feedback.

REFERENCES

Josh Achiam, Steven Adler, Sandhini Agarwal, Lama Ahmad, Ilge Akkaya, Florencia Leoni Aleman, Diogo Almeida, Janko Altschmidt, Sam Altman, Shyamal Anadkat, et al. Gpt-4 technical report. *arXiv preprint*

- 540 *arXiv:2303.08774*, 2023.
- 541
- 542 Jean-Yves Audibert and Sébastien Bubeck. Best arm identification in multi-armed bandits. In *Conference on*
543 *learning theory*, pp. 41–53, 2010.
- 544 Peter Auer, Nicolò Cesa-Bianchi, and Paul Fischer. Finite-time analysis of the multiarmed bandit problem.
545 *Machine Learning*, 47:235–256, 2002.
- 546 Mohammad Gheshlaghi Azar, Zhaohan Daniel Guo, Bilal Piot, Remi Munos, Mark Rowland, Michal Valko,
547 and Daniele Calandriello. A general theoretical paradigm to understand learning from human preferences.
548 In *International Conference on Artificial Intelligence and Statistics*, pp. 4447–4455. PMLR, 2024.
- 549
- 550 Yuntao Bai, Andy Jones, Kamal Ndousse, Amanda Askell, Anna Chen, Nova DasSarma, Dawn Drain, Stanislav
551 Fort, Deep Ganguli, Tom Henighan, et al. Training a helpful and harmless assistant with reinforcement
552 learning from human feedback. *arXiv preprint arXiv:2204.05862*, 2022.
- 553 Christopher Berner, Greg Brockman, Brooke Chan, Vicki Cheung, Przemysław Dębiak, Christy Dennison,
554 David Farhi, Quirin Fischer, Shariq Hashme, Chris Hesse, et al. Dota 2 with large scale deep reinforcement
555 learning. *arXiv preprint arXiv:1912.06680*, 2019.
- 556 Stella Biderman, Hailey Schoelkopf, Quentin Gregory Anthony, Herbie Bradley, Kyle O’Brien, Eric Hallahan,
557 Mohammad Aflah Khan, Shivanshu Purohit, USVSN Sai Prashanth, Edward Raff, et al. Pythia: A suite
558 for analyzing large language models across training and scaling. In *International Conference on Machine*
559 *Learning*, pp. 2397–2430. PMLR, 2023.
- 560 Ralph Allan Bradley and Milton E. Terry. Rank analysis of incomplete block designs: I. the method of paired
561 comparisons. *Biometrika*, 39(3/4):324–345, 1952.
- 562 Sébastien Bubeck, Rémi Munos, and Gilles Stoltz. Pure exploration in multi-armed bandits problems. In
563 *Algorithmic Learning Theory: 20th International Conference, ALT 2009, Porto, Portugal, October 3-5,*
564 *2009. Proceedings 20*, pp. 23–37. Springer, 2009.
- 565
- 566 Sébastien Bubeck, Varun Chandrasekaran, Ronen Eldan, Johannes Gehrke, Eric Horvitz, Ece Kamar, Peter Lee,
567 Yin Tat Lee, Yuanzhi Li, Scott Lundberg, et al. Sparks of artificial general intelligence: Early experiments
568 with gpt-4. *arXiv preprint arXiv:2303.12712*, 2023.
- 569 Róbert Busa-Fekete, Balázs Szörényi, Paul Weng, Weiwei Cheng, and Eyke Hüllermeier. Preference-based re-
570 inforcement learning: evolutionary direct policy search using a preference-based racing algorithm. *Machine*
571 *learning*, 97:327–351, 2014.
- 572 Olivier Chapelle and Lihong Li. An empirical evaluation of thompson sampling. *Advances in neural informa-*
573 *tion processing systems*, 24, 2011.
- 574 OpenAI ChatGPT. ChatGPT. <https://chatgpt.com/>, 2024. Accessed: 2024-09-30.
- 575
- 576 Changyu Chen, Zichen Liu, Chao Du, Tianyu Pang, Qian Liu, Arunesh Sinha, Pradeep Varakantham, and Min
577 Lin. Bootstrapping language models with dpo implicit rewards. *arXiv preprint arXiv:2406.09760*, 2024.
- 578 Paul F Christiano, Jan Leike, Tom Brown, Miljan Martic, Shane Legg, and Dario Amodei. Deep reinforcement
579 learning from human preferences. *Advances in neural information processing systems*, 30, 2017.
- 580 Ganqu Cui, Lifan Yuan, Ning Ding, Guanming Yao, Wei Zhu, Yuan Ni, Guotong Xie, Zhiyuan Liu, and
581 Maosong Sun. Ultrafeedback: Boosting language models with high-quality feedback, 2023.
- 582
- 583 Nirjhar Das, Souradip Chakraborty, Aldo Pacchiano, and Sayak Ray Chowdhury. Provably sample efficient
584 rlhf via active preference optimization. *arXiv preprint arXiv:2402.10500*, 2024.
- 585 Hanze Dong, Wei Xiong, Bo Pang, Haoxiang Wang, Han Zhao, Yingbo Zhou, Nan Jiang, Doyen Sahoo,
586 Caiming Xiong, and Tong Zhang. Rlhf workflow: From reward modeling to online rlhf. *arXiv preprint*
587 *arXiv:2405.07863*, 2024.
- 588 Yann Dubois, Balázs Galambosi, Percy Liang, and Tatsunori B Hashimoto. Length-controlled alpacaeval: A
589 simple way to debias automatic evaluators. *arXiv preprint arXiv:2404.04475*, 2024.
- 590 Miroslav Dudík, Katja Hofmann, Robert E Schapire, Aleksandrs Slivkins, and Masrour Zoghi. Contextual
591 dueling bandits. In *Conference on Learning Theory*, pp. 563–587. PMLR, 2015.
- 592
- 593 Vikranth Dwaracherla, Seyed Mohammad Asghari, Botao Hao, and Benjamin Van Roy. Efficient exploration
for llms. In *International Conference on Machine Learning*, 2024.

- 594 Lasse Espeholt, Hubert Soyer, Remi Munos, Karen Simonyan, Vlad Mnih, Tom Ward, Yotam Doron, Vlad
595 Firoiu, Tim Harley, Iain Dunning, et al. Impala: Scalable distributed deep-rl with importance weighted
596 actor-learner architectures. In *International conference on machine learning*, pp. 1407–1416. PMLR, 2018.
- 597 Javier González, Zhenwen Dai, Andreas Damianou, and Neil D Lawrence. Preferential bayesian optimization.
598 In *International Conference on Machine Learning*, pp. 1282–1291. PMLR, 2017.
- 599 Shangmin Guo, Biao Zhang, Tianlin Liu, Tianqi Liu, Misha Khalman, Felipe Llinares, Alexandre Rame,
600 Thomas Mesnard, Yao Zhao, Bilal Piot, et al. Direct language model alignment from online ai feedback.
601 *arXiv preprint arXiv:2402.04792*, 2024.
- 602 Fredrik K Gustafsson, Martin Danelljan, and Thomas B Schon. Evaluating scalable bayesian deep learning
603 methods for robust computer vision. In *Proceedings of the IEEE/CVF conference on computer vision and
604 pattern recognition workshops*, pp. 318–319, 2020.
- 605 Jian Hu, Xibin Wu, Weixun Wang, Dehao Zhang, Yu Cao, et al. Openrlhf: An easy-to-use, scalable and
606 high-performance rlhf framework. *arXiv preprint arXiv:2405.11143*, 2024.
- 607 Shengyi Huang, Michael Noukhovitch, Arian Hosseini, Kashif Rasul, Weixun Wang, and Lewis Tunstall.
608 The n+ implementation details of rlhf with ppo: A case study on tl; dr summarization. *arXiv preprint
609 arXiv:2403.17031*, 2024.
- 610 Michael Janner, Justin Fu, Marvin Zhang, and Sergey Levine. When to trust your model: Model-based policy
611 optimization. *Advances in neural information processing systems*, 32, 2019.
- 612 Natasha Jaques, Judy Hanwen Shen, Asma Ghandeharioun, Craig Ferguson, Agata Lapedriza, Noah Jones,
613 Shixiang Shane Gu, and Rosalind Picard. Human-centric dialog training via offline reinforcement learning.
614 *arXiv preprint arXiv:2010.05848*, 2020.
- 615 Dongfu Jiang, Xiang Ren, and Bill Yuchen Lin. Llm-blender: Ensembling large language models with pair-
616 wise comparison and generative fusion. In *Proceedings of the 61th Annual Meeting of the Association for
617 Computational Linguistics (ACL 2023)*, 2023.
- 618 Julian Katz-Samuels, Lalit Jain, Kevin G Jamieson, et al. An empirical process approach to the union bound:
619 Practical algorithms for combinatorial and linear bandits. *Advances in Neural Information Processing Sys-
620 tems*, 33:10371–10382, 2020.
- 621 Rahul Kidambi, Aravind Rajeswaran, Praneeth Netrapalli, and Thorsten Joachims. Morel: Model-based offline
622 reinforcement learning. *Advances in neural information processing systems*, 33:21810–21823, 2020.
- 623 Woosuk Kwon, Zhuohan Li, Siyuan Zhuang, Ying Sheng, Lianmin Zheng, Cody Hao Yu, Joseph E. Gonzalez,
624 Hao Zhang, and Ion Stoica. Efficient memory management for large language model serving with pagedat-
625 tention. In *Proceedings of the ACM SIGOPS 29th Symposium on Operating Systems Principles*, 2023.
- 626 Balaji Lakshminarayanan, Alexander Pritzel, and Charles Blundell. Simple and scalable predictive uncertainty
627 estimation using deep ensembles. *Advances in neural information processing systems*, 30, 2017.
- 628 Nathan Lambert, Valentina Pyatkin, Jacob Morrison, LJ Miranda, Bill Yuchen Lin, Khyathi Chandu, Nouha
629 Dziri, Sachin Kumar, Tom Zick, Yejin Choi, Noah A. Smith, and Hannaneh Hajishirzi. Rewardbench:
630 Evaluating reward models for language modeling, 2024.
- 631 Sascha Lange, Thomas Gabel, and Martin Riedmiller. Batch reinforcement learning. In *Reinforcement learn-
632 ing: State-of-the-art*, pp. 45–73. Springer, 2012.
- 633 Sergey Levine, Aviral Kumar, George Tucker, and Justin Fu. Offline reinforcement learning: Tutorial, review,
634 and perspectives on open problems. *arXiv preprint arXiv:2005.01643*, 2020.
- 635 Xuechen Li, Tianyi Zhang, Yann Dubois, Rohan Taori, Ishaan Gulrajani, Carlos Guestrin, Percy Liang, and
636 Tatsunori B. Hashimoto. AlpacaEval: An automatic evaluator of instruction-following models. https://github.com/tatsu-lab/alpaca_eval, 5 2023.
- 637 Xuheng Li, Heyang Zhao, and Quanquan Gu. Feel-good thompson sampling for contextual dueling bandits.
638 *arXiv preprint arXiv:2404.06013*, 2024.
- 639 Chris Yuhao Liu, Liang Zeng, Liu Jiakai, Rui Yan, Jujie He, Chaojie Wang, Shuicheng Yan, Yang Liu, and
640 Yuhui Zhou. Skywork reward model series. *arXiv preprint arXiv:2410.18451*, 2024a.
- 641 Zichen Liu, Siyi Li, Wee Sun Lee, Shuicheng Yan, and Zhongwen Xu. Efficient offline policy optimization
642 with a learned model. In *International Conference on Learning Representations*, 2023.

- 648 Zichen Liu, Chao Du, Wee Sun Lee, and Min Lin. Locality sensitive sparse encoding for learning world models
649 online. In *International Conference on Learning Representations*, 2024b.
- 650
- 651 Xiuyuan Lu and Benjamin Van Roy. Ensemble sampling. *Advances in neural information processing systems*,
652 30, 2017.
- 653 Viraj Mehta, Vikramjeet Das, Ojash Neopane, Yijia Dai, Ilija Bogunovic, Jeff Schneider, and Willie
654 Neiswanger. Sample efficient reinforcement learning from human feedback via active exploration. *arXiv*
655 *preprint arXiv:2312.00267*, 2023.
- 656 Luckeciano C Melo, Panagiotis Tigas, Alessandro Abate, and Yarin Gal. Deep bayesian active learning for
657 preference modeling in large language models. *arXiv preprint arXiv:2406.10023*, 2024.
- 658
- 659 Yu Meng, Mengzhou Xia, and Danqi Chen. Simpo: Simple preference optimization with a reference-free
660 reward. *arXiv preprint arXiv:2405.14734*, 2024.
- 661 William Muldrew, Peter Hayes, Mingtian Zhang, and David Barber. Active preference learning for large lan-
662 guage models. In *International Conference on Machine Learning*, 2024.
- 663 Reiichiro Nakano, Jacob Hilton, Suchir Balaji, Jeff Wu, Long Ouyang, Christina Kim, Christopher Hesse,
664 Shantanu Jain, Vineet Kosaraju, William Saunders, et al. Webgpt: Browser-assisted question-answering
665 with human feedback. *arXiv preprint arXiv:2112.09332*, 2021.
- 666
- 667 Andrew Y Ng and Stuart Russell. Algorithms for inverse reinforcement learning. In *International Conference*
668 *on Machine Learning*, volume 1, pp. 2, 2000.
- 669 Long Ouyang, Jeffrey Wu, Xu Jiang, Diogo Almeida, Carroll Wainwright, Pamela Mishkin, Chong Zhang,
670 Sandhini Agarwal, Katarina Slama, Alex Ray, et al. Training language models to follow instructions with
671 human feedback. *Advances in neural information processing systems*, 35:27730–27744, 2022.
- 672 Xue Bin Peng, Aviral Kumar, Grace Zhang, and Sergey Levine. Advantage-weighted regression: Simple and
673 scalable off-policy reinforcement learning. *arXiv preprint arXiv:1910.00177*, 2019.
- 674
- 675 Jan Peters and Stefan Schaal. Reinforcement learning by reward-weighted regression for operational space
676 control. In *International Conference on Machine Learning*, pp. 745–750, 2007.
- 677 Moritz Philipp and Nishihara Robert. Plasma: A high-performance shared-memory object store, 2017. URL
678 <https://arrow.apache.org/blog/2017/08/08/plasma-in-memory-object-store/>.
- 679 Chao Qin, Zheng Wen, Xiuyuan Lu, and Benjamin Van Roy. An analysis of ensemble sampling. *Advances in*
680 *Neural Information Processing Systems*, 35:21602–21614, 2022.
- 681
- 682 Rafael Rafailov, Archit Sharma, Eric Mitchell, Christopher D Manning, Stefano Ermon, and Chelsea Finn.
683 Direct preference optimization: Your language model is secretly a reward model. *Advances in Neural Infor-*
684 *mation Processing Systems*, 37, 2023.
- 685 Rafael Rafailov, Joey Hejna, Ryan Park, and Chelsea Finn. From r to q*: Your language model is secretly a
686 q-function. In *Conference on Language Modeling*, 2024.
- 687
- 688 Samyam Rajbhandari, Jeff Rasley, Olatunji Ruwase, and Yuxiong He. Zero: Memory optimizations toward
689 training trillion parameter models. In *SC20: International Conference for High Performance Computing,*
690 *Networking, Storage and Analysis*, pp. 1–16. IEEE, 2020.
- 691
- 692 Jeff Rasley, Samyam Rajbhandari, Olatunji Ruwase, and Yuxiong He. Deepspeed: System optimizations enable
693 training deep learning models with over 100 billion parameters. In *Proceedings of the 26th ACM SIGKDD*
694 *International Conference on Knowledge Discovery & Data Mining*, pp. 3505–3506, 2020.
- 695
- 696 Herbert Robbins. Some aspects of the sequential design of experiments. *Bulletin of the American Mathematics*
697 *Society*, 58:527–535, 1952.
- 698
- 699 Daniel Russo. Simple bayesian algorithms for best arm identification. In *Conference on Learning Theory*, pp.
700 1417–1418. PMLR, 2016.
- 701 Daniel J Russo, Benjamin Van Roy, Abbas Kazerouni, Ian Osband, Zheng Wen, et al. A tutorial on thompson
sampling. *Foundations and Trends® in Machine Learning*, 11(1):1–96, 2018.
- Aadirupa Saha. Optimal algorithms for stochastic contextual preference bandits. *Advances in Neural Informa-*
tion Processing Systems, 34:30050–30062, 2021.

- 702 Julian Schrittwieser, Thomas Hubert, Amol Mandhane, Mohammadamin Barekatin, Ioannis Antonoglou, and
703 David Silver. Online and offline reinforcement learning by planning with a learned model. *Advances in*
704 *Neural Information Processing Systems*, 34:27580–27591, 2021.
- 705 John Schulman, Filip Wolski, Prafulla Dhariwal, Alec Radford, and Oleg Klimov. Proximal policy optimization
706 algorithms. *arXiv preprint arXiv:1707.06347*, 2017.
- 707 Nisan Stiennon, Long Ouyang, Jeffrey Wu, Daniel Ziegler, Ryan Lowe, Chelsea Voss, Alec Radford, Dario
708 Amodei, and Paul F Christiano. Learning to summarize with human feedback. *Advances in Neural Infor-*
709 *mation Processing Systems*, 33:3008–3021, 2020.
- 710 Richard S. Sutton. Integrated architectures for learning, planning, and reacting based on approximating dy-
711 namic programming. In *Machine Learning Proceedings*, pp. 216–224. Morgan Kaufmann, 1990.
- 712 Richard S. Sutton and Andrew G. Barto. *Reinforcement Learning: An Introduction*. The MIT Press, second
713 edition, 2018.
- 714 Richard S Sutton, Michael Bowling, and Patrick M Pilarski. The alberta plan for ai research. *arXiv preprint*
715 *arXiv:2208.11173*, 2022.
- 716 Fahim Tajwar, Anikait Singh, Archit Sharma, Rafael Rafailov, Jeff Schneider, Tengyang Xie, Stefano Ermon,
717 Chelsea Finn, and Aviral Kumar. Preference fine-tuning of llms should leverage suboptimal, on-policy data.
718 *arXiv preprint arXiv:2404.14367*, 2024.
- 719 Yunhao Tang, Daniel Zhaohan Guo, Zeyu Zheng, Daniele Calandriello, Yuan Cao, Eugene Tarassov, Rémi
720 Munos, Bernardo Ávila Pires, Michal Valko, Yong Cheng, et al. Understanding the performance gap between
721 online and offline alignment algorithms. *arXiv preprint arXiv:2405.08448*, 2024.
- 722 William R Thompson. On the likelihood that one unknown probability exceeds another in view of the evidence
723 of two samples. *Biometrika*, 25(3-4):285–294, 1933.
- 724 Hugo Touvron, Louis Martin, Kevin Stone, Peter Albert, Amjad Almahairi, Yasmine Babaei, Nikolay Bash-
725 lykov, Soumya Batra, Prajjwal Bhargava, Shrubti Bhosale, et al. Llama 2: Open foundation and fine-tuned
726 chat models. *arXiv preprint arXiv:2307.09288*, 2023.
- 727 Ashish Vaswani, Noam Shazeer, Niki Parmar, Jakob Uszkoreit, Llion Jones, Aidan N Gomez, Łukasz Kaiser,
728 and Illia Polosukhin. Attention is all you need. In *Advances in Neural Information Processing Systems*,
729 volume 30, 2017.
- 730 Haoxiang Wang, Wei Xiong, Tengyang Xie, Han Zhao, and Tong Zhang. Interpretable preferences via multi-
731 objective reward modeling and mixture-of-experts. *arXiv preprint arXiv:2406.12845*, 2024.
- 732 Jiayi Weng, Min Lin, Shengyi Huang, Bo Liu, Denys Makoviichuk, Viktor Makoviychuk, Zichen Liu, Yufan
733 Song, Ting Luo, Yukun Jiang, Zhongwen Xu, and Shuicheng Yan. EnvPool: A highly parallel reinforcement
734 learning environment execution engine. In *Advances in Neural Information Processing Systems*, volume 35,
735 pp. 22409–22421, 2022.
- 736 Ronald J Williams. Simple statistical gradient-following algorithms for connectionist reinforcement learning.
737 *Machine learning*, 8:229–256, 1992.
- 738 Christian Wirth, Riad Akrou, Gerhard Neumann, and Johannes Fürnkranz. A survey of preference-based
739 reinforcement learning methods. *Journal of Machine Learning Research*, 18(136):1–46, 2017.
- 740 Huasen Wu and Xin Liu. Double thompson sampling for dueling bandits. *Advances in neural information*
741 *processing systems*, 29, 2016.
- 742 Tengyang Xie, Dylan J Foster, Akshay Krishnamurthy, Corby Rosset, Ahmed Awadallah, and Alexander
743 Rakhlin. Exploratory preference optimization: Harnessing implicit q*-approximation for sample-efficient
744 rlhf. *arXiv preprint arXiv:2405.21046*, 2024.
- 745 Wei Xiong, Hanze Dong, Chenlu Ye, Ziqi Wang, Han Zhong, Heng Ji, Nan Jiang, and Tong Zhang. Iterative
746 preference learning from human feedback: Bridging theory and practice for rlhf under kl-constraint. In
747 *Forty-first International Conference on Machine Learning*, 2024.
- 748 Jing Xu, Andrew Lee, Sainbayar Sukhbaatar, and Jason Weston. Some things are more cringe than others:
749 Preference optimization with the pairwise cringe loss. *arXiv preprint arXiv:2312.16682*, 2023.
- 750 Fan Yang, Gabriel Barth-Maron, Piotr Stańczyk, Matthew Hoffman, Siqi Liu, Manuel Kroiss, Aedan Pope,
751 and Alban Rrustemi. Launchpad: A programming model for distributed machine learning research. *arXiv*
752 *preprint arXiv:2106.04516*, 2021a.

756 Keming Yang, Zichen Liu, and Philip Cheng. MOSEC: Model Serving made Efficient in the Cloud. <https://github.com/mosecorg/mosec>, 2021b.
757
758

759 Tianhe Yu, Aviral Kumar, Rafael Rafailov, Aravind Rajeswaran, Sergey Levine, and Chelsea Finn. Combo:
760 Conservative offline model-based policy optimization. *Advances in neural information processing systems*,
761 34:28954–28967, 2021.

762 Yisong Yue, Josef Broder, Robert Kleinberg, and Thorsten Joachims. The k-armed dueling bandits problem.
763 *Journal of Computer and System Sciences*, 78(5):1538–1556, 2012.

764 Shenao Zhang, Donghan Yu, Hiteshi Sharma, Ziyi Yang, Shuohang Wang, Hany Hassan, and Zhaoran
765 Wang. Self-exploring language models: Active preference elicitation for online alignment. *arXiv preprint*
766 *arXiv:2405.19332*, 2024a.

767 Xuan Zhang, Chao Du, Tianyu Pang, Qian Liu, Wei Gao, and Min Lin. Chain of preference optimization:
768 Improving chain-of-thought reasoning in llms. *Advances in Neural Information Processing Systems*, 38,
769 2024b.

770 Yao Zhao, Rishabh Joshi, Tianqi Liu, Misha Khalman, Mohammad Saleh, and Peter J Liu. Slic-hf: Sequence
771 likelihood calibration with human feedback. *arXiv preprint arXiv:2305.10425*, 2023.
772

773 Lianmin Zheng, Wei-Lin Chiang, Ying Sheng, Siyuan Zhuang, Zhanghao Wu, Yonghao Zhuang, Zi Lin, Zhuo-
774 han Li, Dacheng Li, Eric Xing, et al. Judging llm-as-a-judge with mt-bench and chatbot arena. *Advances in*
775 *Neural Information Processing Systems*, 36:46595–46623, 2023.

776 Banghua Zhu, Michael Jordan, and Jiantao Jiao. Principled reinforcement learning with human feedback from
777 pairwise or k-wise comparisons. In *Proceedings of the 40th International Conference on Machine Learning*,
778 pp. 43037–43067. PMLR, 2023.

779 Yinglun Zhu, Dylan J Foster, John Langford, and Paul Mineiro. Contextual bandits with large action spaces:
780 Made practical. In *International Conference on Machine Learning*, pp. 27428–27453. PMLR, 2022.
781
782
783
784
785
786
787
788
789
790
791
792
793
794
795
796
797
798
799
800
801
802
803
804
805
806
807
808
809

A ALGORITHM DETAILS

While Algorithm 1 presents our Thompson sampling algorithm for LLM alignment, it is intractable and centered around the reward posterior modeling. We next present a practical sample-efficient alignment agent that learns both an LLM policy and an epistemic reward model online.

general:add-
details

fdal

Algorithm 2 Sample-efficient alignment (SEA) for LLMs

Input: Reference policy π_{ref} , DAP loss function F , prompt distribution $p_{\mathcal{X}}$, unknown but queryable preference oracle \mathbb{P} , mixture ratio γ .

- 1: Initialize experience $\mathcal{D}_0 \leftarrow \emptyset$, policy $\pi_{\theta^0} \leftarrow \pi_{\text{ref}}$, and ERM weights $\Phi^0 = \{\phi_k^0\}_{k=1}^K$ randomly.
 - 2: **for** $t = 1, \dots, T$ **do**
 - 3: Receive a prompt $\mathbf{x}_t \sim p_{\mathcal{X}}$.
 - 4: Sample M responses $\mathbf{y}_t^i \sim \pi_{\theta^{t-1}}(\cdot | \mathbf{x}_t)$ to construct $\mathcal{S}_t = \{\mathbf{y}_t^i\}_{i=1}^M$.
 - 5: Sample $\phi \sim \text{Uniform}(\Phi^{t-1})$ and set $\mathbf{y}_t \leftarrow \arg \max_{\mathbf{b} \in \mathcal{S}_t} r_{\phi}(\mathbf{x}_t, \mathbf{b})$. // Select 1st response \mathbf{y} .
 - 6: **repeat**
 - 7: Sample $\phi \sim \text{Uniform}(\Phi^{t-1})$ and set $\mathbf{y}'_t \leftarrow \arg \max_{\mathbf{b} \in \mathcal{S}_t} r_{\phi}(\mathbf{x}_t, \mathbf{b})$. // Select 2nd response \mathbf{y}' .
 - 8: **until** $\mathbf{y}'_t \neq \mathbf{y}_t$
 - 9: // BAI objective: labeling via crowdsourcing.
 - 10: Set $\mathbf{y}'_t \leftarrow \arg \max_{\mathbf{b} \in \mathcal{S}_t} \mathbb{V}_{\phi} [\sigma(r_{\phi}(\mathbf{x}_t, \mathbf{y}_t) - r_{\phi}(\mathbf{x}_t, \mathbf{b}))]$, // OR select 2nd response \mathbf{y}' .
 where $\mathbb{V}_{\phi}[\cdot]$ computes variance across ensemble members of Φ^{t-1} .
 - 11: **if** $g < \gamma$ for $g \sim \text{Uniform}(0, 1)$ **then**
 - 12: Label $\{\mathbf{y}_t, \mathbf{y}'_t\}$ with \mathbb{P} to obtain $\mathcal{B}_t = \{(\mathbf{x}_t, \mathbf{y}_t^+, \mathbf{y}_t^-)\}$ and update experience $\mathcal{D}_t \leftarrow \mathcal{D}_{t-1} \cup \mathcal{B}_t$.
 - 13: **else**
 - 14: Use $\mathcal{R}_{\Phi^{t-1}}$ to get synthetic labels and obtain $\mathcal{B}_t = \{(\mathbf{x}_t, \tilde{\mathbf{y}}_t^+, \tilde{\mathbf{y}}_t^-)\}$.
 - 15: **end if**
 - 16: Update ERM with the regularized NLL loss (Eq. (8)):

$$\Phi^t \leftarrow \Phi^{t-1} - \alpha_{\mathcal{R}} \nabla_{\Phi} \mathcal{L}_{\mathcal{R}}(\Phi^{t-1} | \mathcal{D}_t).$$
// Reward learning.
 - 17: Update policy with the direct optimizer (Eq. (9)):

$$\theta^t \leftarrow \theta^{t-1} - \alpha_{\pi} \nabla_{\theta} \mathcal{L}_{\pi}(\theta^{t-1} | \mathcal{B}_t, \pi_{\text{ref}}, F).$$
// Policy learning.
 - 18: **end for**
-

In Algorithm 2, we describe an online setting where a single example is processed at each time t (batch size $b = 1$). This is mainly for notational convenience, while in implementation we set b to be the training batch size (e.g., 128). We instantiate the reward posterior with an epistemic reward model, which allows for efficient incremental update and sampling. We also replace the global optimization ($\arg \max_{\mathbf{b} \in \mathcal{Y}}$) with a policy-guided local search among proposals sampled from the latest online policy $\pi_{\theta^{t-1}}$. At each time t , we update ERM weights Φ with m gradient steps with randomly sampled batches from the experience \mathcal{D}_t . We find setting $m = 5$ suffices to achieve a reasonable accuracy. The policy parameters θ are updated using mixed preference data, with a γ proportion being the real environment experience and the remaining $(1 - \gamma)$ from the ERM's synthetic experience. Note that the synthetic experience is not added into \mathcal{D}_t to ensure reward learning always uses ground truth environment data.

We consider the following three direct optimizers in our experiments:

- DPO (Rafailov et al., 2023):

$$F_{\theta}(\mathbf{x}, \mathbf{y}^+, \mathbf{y}^-, \pi_{\text{ref}}) = -\log \sigma \left(\beta \log \frac{\pi_{\theta}(\mathbf{y}^+ | \mathbf{x}) \pi_{\text{ref}}(\mathbf{y}^- | \mathbf{x})}{\pi_{\text{ref}}(\mathbf{y}^+ | \mathbf{x}) \pi_{\theta}(\mathbf{y}^- | \mathbf{x})} \right) \quad (10)$$

- IPO (Azar et al., 2024):

$$F_{\theta}(\mathbf{x}, \mathbf{y}^+, \mathbf{y}^-, \pi_{\text{ref}}) = \left(\log \left(\frac{\pi_{\theta}(\mathbf{y}^+ | \mathbf{x}) \pi_{\text{ref}}(\mathbf{y}^- | \mathbf{x})}{\pi_{\text{ref}}(\mathbf{y}^+ | \mathbf{x}) \pi_{\theta}(\mathbf{y}^- | \mathbf{x})} \right) - \frac{1}{2\beta} \right)^2 \quad (11)$$

- SLiC (Zhao et al., 2023):

$$F_{\theta}(\mathbf{x}, \mathbf{y}^+, \mathbf{y}^-, \pi_{\text{ref}}) = \max \left(0, 1 - \beta \log \frac{\pi_{\theta}(\mathbf{y}^+ | \mathbf{x}) \pi_{\text{ref}}(\mathbf{y}^- | \mathbf{x})}{\pi_{\text{ref}}(\mathbf{y}^+ | \mathbf{x}) \pi_{\theta}(\mathbf{y}^- | \mathbf{x})} \right) \quad (12)$$

where β controls the rate of deviation of π_{θ} from π_{ref} .

B ON CONNECTIONS WITH SINGLE-STEP RL

general

By viewing contextual dueling bandits as *single-step* preference-based RL (PbRL) (Busa-Fekete et al., 2014; Wirth et al., 2017) problems, we can interpret paradigms shown in Figure 3 from the RL perspective.

RLHF approaches (Figure 3a) are instances of **offline model-based RL** (Kidambi et al., 2020; Yu et al., 2021; Schrittwieser et al., 2021; Liu et al., 2023; Tajwar et al., 2024), where they learn a reward model (no need for a transition model since the prompt-response interaction is single-step) of the environment from a batch of offline collected data, and train a policy (i.e., LLM) to maximize the return (i.e., expected one-step reward) with respect to the *learned* reward.

fdal

In contrast, DAP methods (Figure 3b) are similar to **policy-based model-free RL** algorithms, e.g., REINFORCE (Williams, 1992) which conducts policy gradient update:

$$\mathbb{E}_{\mathbf{x} \sim \mathcal{X}} \mathbb{E}_{\mathbf{y} \sim \pi_{\theta}(\cdot|\mathbf{x})} [R(\mathbf{x}, \mathbf{y}) \nabla_{\theta} \log \pi_{\theta}(\mathbf{y}|\mathbf{x})], \quad (13)$$

where $R(\mathbf{x}, \mathbf{y})$ is the return (i.e., cumulative reward) of the trajectory. To connect with DAP, we could set R as arbitrary scalar values based on the binary preference outcomes, e.g., $R(\mathbf{x}, \mathbf{y}^+) = \zeta$ and $R(\mathbf{x}, \mathbf{y}^-) = -\zeta$ for preference triplet $\{\mathbf{x}, \mathbf{y}^+, \mathbf{y}^-\}$. In this way we could rewrite Eq. (13) as

$$\mathbb{E}_{\mathbf{x} \sim \mathcal{X}} \mathbb{E}_{\mathbf{y}, \mathbf{y}' \sim \pi_{\theta}(\cdot|\mathbf{x})} \mathbb{E}_{(\mathbf{y}^+, \mathbf{y}^-) \sim \mathbb{P}} [\zeta (\nabla_{\theta} \log \pi_{\theta}(\mathbf{y}^+|\mathbf{x}) - \nabla_{\theta} \log \pi_{\theta}(\mathbf{y}^-|\mathbf{x}))], \quad (14)$$

by repeating action sampling twice and querying the oracle for preference labeling. This matches the gradient direction of contrastive DAP losses (e.g., see Section 4 of DPO (Rafailov et al., 2023)) if we optimize them online (Guo et al., 2024).

Additionally, active reward learning from behavior policy’s data distribution (Figure 3c) can be regarded as **inverse RL** (Ng & Russell, 2000), which tries to recover environment’s reward function given expert trajectories. In the context of LLM alignment, the preference data $\{\mathbf{x}, \mathbf{y}^+, \mathbf{y}^-\}_{i=1}^N$ directly encodes human’s implicit reward r^* , which can be inversely learned with assumptions such as the BT model (Bradley & Terry, 1952). However, existing methods belonging to this paradigm mostly rely on a fixed (and suboptimal) behavior policy for response sampling, whose coverage inherently limits the quality of the recovered reward function.

Last but not least, **SEA** depicted in Figure 3d resembles a class of **online model-based RL** algorithms, known as Dyna (Sutton, 1990; Janner et al., 2019), that learns a *world model* from environment experience and trains a base agent (consisting of reactive policies and value functions) from both environment experience and model experience. Compared to model-free methods, Dyna naturally enables more sample-efficient learning by planning with the learned world model to update the base agent. In **SEA**, we learn the reward model online and update the LLM (i.e., the reactive policy) with model-planning experience by mixed preference learning (Section 4.2.3). Online model-based RL algorithms could suffer from catastrophic forgetting in the face of nonstationary data (Liu et al., 2024b), and we leave it for future work. Overall, this model-based RL formulation is powerful and explains popular LLM techniques, e.g., Best-of-N sampling (Touvron et al., 2023) can be viewed as planning for acting, which trades compute for performance. We believe it is a promising path leading us to unlock superhuman capabilities of LLMs.

C BASELINE METHODS

fdal

We review four baseline methods that are relevant to this work and used for comparisons in our experiments.

Offline DAP. We review DPO (Rafailov et al., 2023), which is a representative work in the direction of Direct Alignment from Preferences (DAP). It simplifies the two-stage pipeline of offline RLHF (Figure 2 (Left)) as a single step of supervised learning (Figure 2 (Middle)) by leveraging the closed-form solution (Peters & Schaal, 2007; Peng et al., 2019) of the RL objective in Eq. (7):

$$\pi_r(\mathbf{y}|\mathbf{x}) = \frac{1}{Z(\mathbf{x})} \pi_{\text{ref}}(\mathbf{y}|\mathbf{x}) \exp\left(\frac{1}{\beta} r(\mathbf{x}, \mathbf{y})\right), \quad (15)$$

where $Z(\mathbf{x})$ normalizes such that $\sum_{\mathbf{y}} \pi_r(\mathbf{y}|\mathbf{x}) = 1$, to reparametrize r as a function of π :

$$r(\mathbf{x}, \mathbf{y}) = \beta \log \frac{\pi_r(\mathbf{y}|\mathbf{x})}{\pi_{\text{ref}}(\mathbf{y}|\mathbf{x})} + \beta \log Z(\mathbf{x}). \quad (16)$$

Consequently, plugging Eq. (16) into the reward model loss (Eq. (5)) yields a contrastive loss that directly optimizes the policy:

$$\min_{\pi_{\theta}} \mathbb{E}_{(\mathbf{x}, \mathbf{y}^+, \mathbf{y}^-) \sim p_{\mathcal{D}}} \left[-\log \sigma \left(\beta \log \frac{\pi_{\theta}(\mathbf{y}^+|\mathbf{x}) \pi_{\text{ref}}(\mathbf{y}^-|\mathbf{x})}{\pi_{\text{ref}}(\mathbf{y}^+|\mathbf{x}) \pi_{\theta}(\mathbf{y}^-|\mathbf{x})} \right) \right], \quad (17)$$

where \mathcal{D} is a pre-collected offline preference dataset.

We also experiment different DAP methods⁶ besides DPO, such as IPO (Azar et al., 2024) and SLiC (Zhao et al., 2023), whose loss functions are shown in Eq. (11) and (12).

Online DAP (Guo et al., 2024). In contrast to the conventional DAP methods that learn a policy from a fixed dataset \mathcal{D} , online DAP proposes to collect on-policy preference data to update the policy online. It first samples responses from the current policy $(\mathbf{y}, \mathbf{y}') \sim \pi_{\theta_t}$, then acquires preference labels to form a batch $\mathcal{B}_t = \{(\mathbf{x}, \mathbf{y}^+, \mathbf{y}^-)\}_{i=1}^b$. One gradient step minimizing the DAP loss over this data batch to get $\pi_{\theta_{t+1}}$, which is used for the next iteration. Such approach not only mitigates the over-fitting issue faced by offline DAP methods (Guo et al., 2024), but also facilitates online interaction (Property 1) with the environment, falling into the second paradigm of CDB solution algorithms (Figure 3b).

Active Preference Learning (APL) (Muldrew et al., 2024). APL follows the online DAP paradigm, but is restricted to DPO due to its reliance on DPO implicit rewards. Two techniques are proposed by APL to actively select both prompts and dueling responses for querying the preference oracle:

1. *Predictive entropy (PE)* for selecting prompts. In this step APL computes a Monte-Carlo estimate of PE for each prompt as $\mathcal{H}_{\pi_{\theta}}(\mathbf{y}|\mathbf{x}) \approx -\sum_{n=1}^N \log \pi_{\theta}(\mathbf{y}_n|\mathbf{x})/N$, where $\mathbf{y}_n \sim \pi_{\theta}(\cdot|\mathbf{x})$ and $\log \pi_{\theta}(\mathbf{y}_n|\mathbf{x})$ is the summation of log probabilities of each token. Then, APL filters a subset of prompts with high PE to form \mathcal{X}_S .
2. *Preference model certainty* for selecting dueling responses. For prompts in \mathcal{X}_S , APL generates many responses for each prompt, then selects the pair with largest reward margin measured as $|\hat{r}(\mathbf{x}_i, \mathbf{y}_i) - \hat{r}(\mathbf{x}_i, \mathbf{y}'_i)|$, where \hat{r} is the DPO implicit reward $\hat{r}(\mathbf{x}, \mathbf{y}) = \beta(\log \pi_{\theta}(\mathbf{y}|\mathbf{x}) - \log \pi_{\text{ref}}(\mathbf{y}|\mathbf{x}))$.

By above two steps, APL actively explores more uncertain prompts and responses in an online DPO paradigm, satisfying both Properties 1 and 2.

Exploratory Preference Optimization (XPO) (Xie et al., 2024). XPO studies LLM alignment in the framework of token-level MDP, and leverages the property that DPO conducts *implicit Q^* -approximation* (Rafailov et al., 2024), so that

$$\beta \log \frac{\pi^*(\mathbf{y}|\mathbf{x})}{\pi_{\text{ref}}(\mathbf{y}|\mathbf{x})} = r^*(\mathbf{x}, \mathbf{y}) - V^*(\mathbf{x}) \quad \forall \mathbf{y}, \quad (18)$$

where V^* is the optimal value function depending only on the prompt \mathbf{x} . XPO incorporates the *implicit (global) optimism* for exploration by overestimating the value $V_{\pi_{\theta}}(\mathbf{x}) = r^*(\mathbf{x}, \mathbf{y}) - \beta \log \frac{\pi_{\theta}(\mathbf{y}|\mathbf{x})}{\pi_{\text{ref}}(\mathbf{y}|\mathbf{x})}$. This is achieved by optimizing the policy with a modified DPO loss:

$$\min_{\pi_{\theta}} \mathbb{E}_{(\mathbf{x}, \mathbf{y}^+, \mathbf{y}^-, \mathbf{y}^{\text{ref}}) \sim p_{\mathcal{B}^t}} \left[\alpha \log \pi_{\theta}(\mathbf{y}^{\text{ref}}|\mathbf{x}) - \log \sigma \left(\beta \log \frac{\pi_{\theta}(\mathbf{y}^+|\mathbf{x}) \pi_{\text{ref}}(\mathbf{y}^-|\mathbf{x})}{\pi_{\text{ref}}(\mathbf{y}^+|\mathbf{x}) \pi_{\theta}(\mathbf{y}^-|\mathbf{x})} \right) \right], \quad (19)$$

where $\mathbf{y}^{\text{ref}} \sim \pi_{\text{ref}}(\cdot|\mathbf{x})$ and \mathcal{B}^t is an on-policy data batch in the same vein as online DPO. Intuitively, the first term in Eq. (19) biases the policy toward a large value estimation such that $V_{\pi_{\theta}} \gtrsim V^*$, implementing the optimism in the face of uncertainty (OFU) for exploration. Theoretically, Xie et al. (2024) also prove the sample complexity bound of XPO, making it a promising algorithm for online LLM alignment.

Self-exploring language model (SELM) (Zhang et al., 2024a) is a concurrent work of Xie et al. (2024) that proposes **nearly the same theoretic algorithm** to achieve OFU. However, the practical implementation of SELM **involves offline preference dataset for training, making it hard to benchmark in an online alignment setting like ours**. Therefore, we will keep XPO as our baseline while omitting the comparison with SELM. cF2f

D FULL EXPERIMENTAL DETAILS

In the main text we focus on the task of summarization using the TL;DR dataset. This provides a lightweight and clean setting to extensively study different algorithmic designs with affordable computational resources. Appendix D.1 provides the full details of this setting.

To further validate the sample efficiency of **SEA** in aligning LLMs to perform general tasks, we adopt the **UltraFeedback dataset** (Cui et al., 2023) and evaluate trained LLMs on **AlpacaEval 2.0** (Li et al., 2023). Appendix D.2 provides more details of this setting. z8J2

D.1 DETAILS OF TL;DR TASK

Models. We experiment three model scales (1B, 2.8B, 6.9B) from the Pythia family (Biderman et al., 2023). We take pretrained SFT models from Huang et al. (2024) as π_{ref} for the starting model in all experiments. Except in Section 6.1, we use 1B model for other experiments to save computation.

⁶We use “DAP method” and “direct optimizer” interchangeably.

Preference oracle. We simulate the process of human feedback with a strong scalar RM and refer it as preference oracle. We choose Skywork-Reward-Llama-3.1-8B⁷ (Liu et al., 2024a), which is top-ranked in RewardBench leaderboard (Lambert et al., 2024), as the preference oracle.

Epistemic reward model. We build ERM on top of a pretrained 0.4B transformer (Jiang et al., 2023), by removing its head and adding an ensemble of MLPs. The size of ensemble is set to $K = 20$, and all MLPs contain 2 hidden layers of 128 nodes. Note that the ERM is chosen to be much smaller than the preference oracle following Dwaracherla et al. (2024), which reflects the fact that human preferences can be more complex than what the agent can model. The regularization coefficient λ is fixed to be 0.5 after a coarse hyperparameter search.

Data. We employ the widely adopted TL;DR dataset (Stiennon et al., 2020) for our experiments. It consists of Reddit posts as prompts, and the agent is required to give summaries that align with human preferences. We fix 50k prompts for training and limit the query budget to 50k as well.

DAP methods. We adopt three DAP methods (direct optimizers) to thoroughly validate our algorithm, including DPO (Rafailov et al., 2023), IPO (Azar et al., 2024) and SLiC (Zhao et al., 2023). **Except in Section 6.1, all experiments are done with DPO as the direct optimizer.**

fdaL

Baselines. Similar to Guo et al. (2024), we include the offline and online variants of different DAP methods as baselines. Additionally, we compare with two active exploration baselines built on online DPO: APL (Muldrup et al., 2024) and XPO (Xie et al., 2024). A detailed review of all baselines can be found in Appendix C.

Metrics. We use the win rate of agent’s responses against reference responses judged by the preference oracle as the performance metric. This metric can reflect both the agent’s cumulative regret and anytime regret (i.e., average performance). In the E&E setting, we measure the “online” win rate of the agent’s dueling responses that are executed during experience collection and take the average. In the BAI setting, we measure the “offline” win rate by evaluating the latest agent’s responses given a fixed set of 1000 holdout prompts periodically. We mainly focus on the BAI setting because crowdsourcing seems a major scenario for most practitioners, and present one set of experiments for comparing different exploration strategies in both settings. When the comparison is only made within a model scale, we report the relative win rate against the initial STF models. When the comparison is across scales (Figure 1 Left), we report the absolute win rate against the ground truth responses in the dataset.

Hyperparameters. We set $\beta = 0.1$ for DPO and $\beta = 0.2$ for SLiC and find they are robust for all scales. We tune β from $\{0.2, 0.3, 0.5, 1.0\}$ for IPO across scales and report the best performing results. We sample $M = 20$ on-policy responses with a temperature $\eta = 0.7$ during training, and use greedy decoding for offline evaluation (BAI’s metric). We use the Adam optimizer with learning rate of 5×10^{-7} and cosine scheduling, and set the batch size to be 128. We initialize the mixture ratio γ of SEA to be 1 and adjust it to 0.7 after a burn-in period of 1k samples.

All hyperparameters are kept the same for offline and online baselines, except that online methods update the sampling policy after every gradient step as the latest π_{θ_t} . For APL and XPO, we keep the learning rate and DPO’s β the same for apple-to-apple comparisons. Specifically for APL, we initially sample 1024 prompts per batch and use the predictive entropy to filter a subset of 128 prompts. Then, we sample 8 responses per prompt and use the preference model certainty to finalize two responses for the duel. Specifically for XPO, we follow the their recommended optimism coefficient to set $\alpha = 5 \times 10^{-6}$.

fdaL

Statistical significance. There are various factors to introduce randomness during online learning. We thus launch 3 independent runs for every experiment with different random seeds. All the results are reported with mean and standard error to indicate their statistical significance.

Computational resources. Experiments at all scales are conducted on a single machine with 8 A100 GPUs to run the learner and actors. We additionally host a separate remote server with workers spawned on 16 A100 GPUs for the oracle RM⁸, so that it can be queried by all concurrently running experiments. All experiments conducted for this research consume about 2 A100 GPU years.

D.2 DETAILS OF GENERAL TASKS

z8J2,RtS4,fdaL

Model. Following Meng et al. (2024); Zhang et al. (2024a), we employ Llama3-8B-Instruct⁹ as our initial model π_{ref} .

Preference oracle. We follow Meng et al. (2024) to adopt ArmoRM-Llama3-8B-v0.1¹⁰ (Wang et al., 2024) as the preference oracle to provide online preference feedback.

⁷<https://huggingface.co/Skywork/Skywork-Reward-Llama-3.1-8B>.

⁸We utilize the Kubernetes service for routing requests to multiple Mosec (Yang et al., 2021b) instances.

⁹<https://huggingface.co/meta-llama/Meta-Llama-3-8B-Instruct>.

¹⁰<https://huggingface.co/RLHFlow/ArmoRM-Llama3-8B-v0.1>.

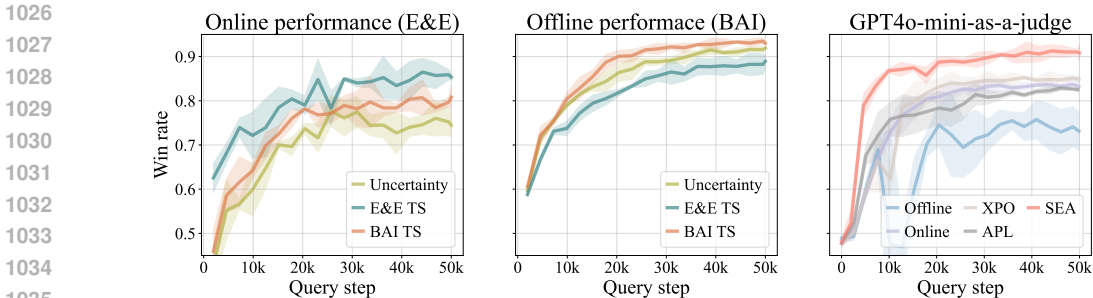


Figure 7: (Left and Middle) Win rate comparison of different exploration strategies measured in E&E and BAI settings. **(Right)** Win rate comparison of different agents when using GPT4o-mini to simulate human feedback via LLM-as-a-judge.

Data. We take the UltraFeedback dataset (Cui et al., 2023), which is widely used for LLM alignment in the literature. We filter out samples whose prompt is longer than 1800 tokens and result in 61k samples. We extract prompts from the filtered dataset while excluding the responses. The prompt set are collected from multiple sources and cover diverse domains, making it suitable to improve LLM’s capability on general tasks.

DAP method and baselines. We employ the state-of-the-art DAP method, SimPO (Meng et al., 2024), as our direct optimizer. Since SimPO is originally an offline algorithm, we extend it to Online SimPO and take both offline and online variants as baselines.

Evaluation. We evaluate SEA and baselines using AlpacaEval 2.0 (Li et al., 2023). It consists of 805 test prompts, and uses GPT4-Turbo to judge the quality of model responses against reference responses generated by GPT-4-Turbo. We follow the standard protocol to report both the win rate (WR) and the Length-Controlled win rate (LC) (Dubois et al., 2024).

Hyperparameters. We follow SimPO’s recommended hyperparameters to set $\beta = 10$ and $\gamma/\beta = 0.3$. We use a learning rate of 8×10^{-7} and batch size of 128. The decoding temperature is set to be 0.9 for generating evaluation outputs. The same hyperparameters apply to baselines and our method. Configurations of SEA are kept the same as those in the TL;DR task (Appendix D.1).

E EXTENDED EMPIRICAL STUDIES

We present additional empirical studies in this section, including investigation on different exploration strategies (Appendix E.1) and preference oracles (Appendix E.2) on the TL;DR task, as well as the performance comparison on AlpacaEval 2.0 for general tasks (Appendix E.3).

E.1 CHOICE OF EXPLORATION STRATEGIES

Recalling that different LLM alignment scenarios (online system or crowdsourcing) require different exploration strategies to meet their respective learning objectives (Section 2.2). We investigate three strategies based on posterior sampling and compare them on both online and offline performance. The first strategy (Uncertainty) focuses on pure exploration with information maximization. It seeks the pair of dueling responses that exhibits the largest epistemic uncertainty, which is implemented by selecting the pair whose logits difference has the largest variance across ensemble members. The second (E&E-TS) and the third (BAI-TS) strategies follow the principles in Algorithm 1, and their differences are between Line 5 and Line 6. The comparison results are shown in Figure 7 (Left and Middle). Focusing on the left plot, we observe that E&E-TS strategy achieves the best online performance, which is within our expectation. In contrast, Uncertainty shows the worst online performance because it tries to maximize the information gain but does not prioritize reward maximization. On the other hand, conclusions are interestingly different when taking the offline performance as the metric. In this case, BAI-TS and Uncertainty both exhibit more efficient offline performance improvement than E&E-TS. This can be attributed to that exploration for uncertainty minimizing helps to identify more informative responses to train the LLM policy. Moreover, BAI-TS \succ Uncertainty indicates exploration with both reward and information maximization is better than exploration with only information maximization. E&E-TS, however, always chooses two responses with similarly high quality to exploit. This can not only lead to less efficient exploration, but also result in less efficient policy learning due to smaller DAP loss gradients.

E.2 ALIGNING LLMs WITH A HUMAN SIMULATOR

Results presented so far are based on experimenting LLM alignment with the preference oracle being a scalar reward model, which is deterministic and does not capture the potential randomness of the choice by real humans. To test different agents in a more realistic setting, we use generative models as human simulator in an LLM-as-a-judge (Bubeck et al., 2023; Zheng et al., 2023) manner. In particular, we directly query the OpenAI

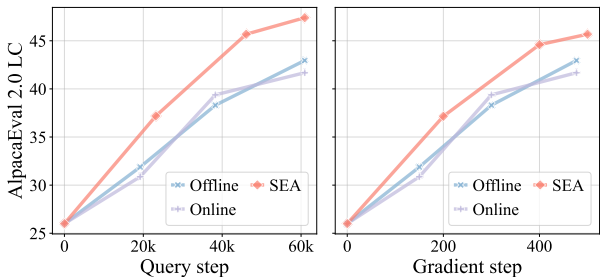


Figure 8: LC win rates on AlpaEval 2.0 with respect to query budget and gradient update budget.

Table 2: AlpaEval 2.0 results. LLM exploration methods are highlighted in blue.

Model	LC	WR
GPT-4 Omni (05/13)	57.5	51.3
GPT-4 Turbo (04/09)	55.0	46.1
Yi-Large Preview	51.9	57.5
SEA+SimPO	47.4	41.1
Claude 3 Opus (02/29)	40.5	26.1
SELM	34.7	34.8
XPO	29.4	-
Llama 3 8B Instruct	22.9	22.6

API and use gpt-4o-mini-2024-07-18 as the judge to provide preference feedback. We use a similar prompt template to Li et al. (2023)’s, which is shown in Figure 11. We also randomly swap the order of two responses to mitigate the known position bias of LLM judges. The results are shown in Figure 7 (Right). We can observe the performance curves generally exhibit higher variance, possibly due to the randomness introduced in the feedback process, which puts more stringent requirements for learning algorithms. The two active exploration methods demonstrate opposite results to those in Section 6.1—APL learns fast initially but is eventually outperformed by Online, while XPO improves over Online after stabilizing its training and delivers a better final performance. Our agent, SEA, is shown to offer the best sample efficiency as well as asymptotic performance, further validating the importance of online learning and well-designed active exploration mechanism.

E.3 PERFORMANCE ON GENERAL TASKS

We investigate the generalizability of SEA by training with the prompt set from UltraFeedback (Cui et al., 2023) and evaluating the model performance on AlpaEval 2.0 (Li et al., 2023). Figure 8 shows the Length-Controlled (LC) win rate of different models against GPT-4-Turbo. The left plot compares the sample efficiency (in terms of the number of queries) of offline, online and SEA SimPO. The results suggest that enabling online interaction does not improve the sample efficiency over the offline counterpart. Such observation is in stark contrast to what we have seen in the TL;DR task, where the online agent always improves over the offline ones. We hypothesize that this is due to the different coverage of π_{ref} in these two tasks. For TL;DR, which is a much easier task, the initial SFT models already have good coverage, permitting online DAP with only passive exploration to work reasonably well; however, for more challenging tasks, the insufficient coverage of π_{ref} would lead to sample complexity exponential in $\frac{1}{\beta}$ (Xie et al., 2024), which necessitates deliberate exploration, such as Thompson sampling proposed in this work. The above claim is justified by observing that SEA largely improves the sample efficiency over the online and offline variants.

Attentive readers may have noticed that comparing query budget could be advantageous to SEA because pseudo labels are used in mixed preference learning (Section 4.2.3), which results in more gradient steps given the same query budget. In the right plot of Figure 8, we show the performance versus gradient step. We can observe SEA has the steepest learning curve, verifying that it explores more informative samples to yield faster improvement.

Last but not least, in Table 2, we show the AlpaEval 2.0 LC win rates of XPO and SELM (as reported in their papers), along with ours and several cutting-edge LLMs. SEA is agnostic to direct optimizers, thus it can leverage the state-of-the-art SimPO to achieve a high LC of 47.4%. On the other hand, XPO and SELM can only be applied to DPO, restricting their potential to incorporate future advances in direct optimization algorithms.

F SYSTEM BENCHMARKING

We conduct a rigorous benchmarking comparison on the efficiency of online DPO training using our learning system, alongside the trl’s implementation¹¹.

Settings. In alignment with the examples provided by trl, we use the TL;DR (Stiennon et al., 2020) dataset and evaluate training efficiency at three model scales: 1B, 2.8B and 6.9B parameters for both SFT-ed LLMs¹²

¹¹https://github.com/huggingface/trl/blob/main/trl/trainer/online_dpo_trainer.py.

¹²<https://huggingface.co/trl-lib/pythia-1b-deduped-tldr-sft>; <https://huggingface.co/trl-lib/pythia-2.8b-deduped-tldr-sft>; <https://huggingface.co/trl-lib/pythia-6.9b-deduped-tldr-sft>

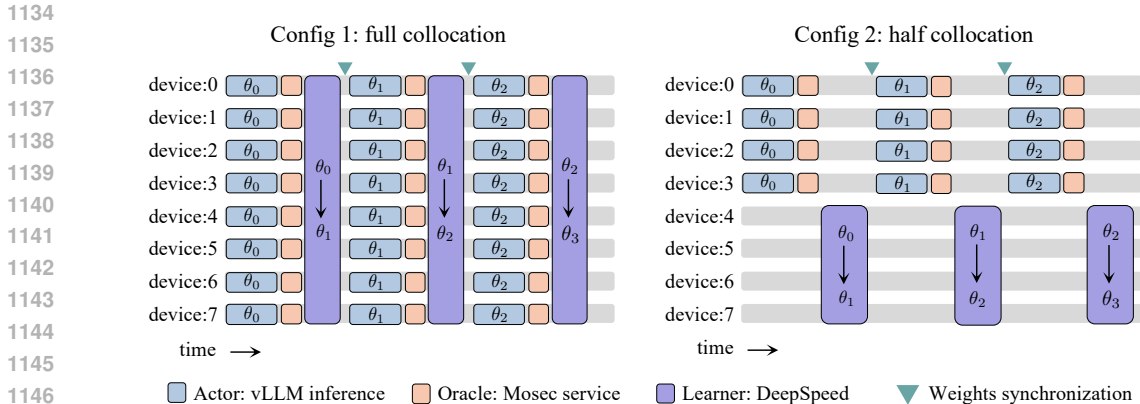


Figure 9: Two example configurations of our learning system used in benchmarking experiments.

and exclusively trained RMs¹³. This is similar to the settings in our experiments (see Appendix D) except that we fix the preference oracle to be a strong general-purpose RM.

Hardware & Software. All benchmarking experiments are conducted on a single machine with eight A100-40G GPUs and 96 AMD EPYC 7352 CPUs. To ensure fair comparison, we align all key hyperparameters for both our codebase and tr1. The DeepSpeed ZeRO-2 strategy is employed by default when GPU memory suffices; otherwise, ZeRO-3 or ZeRO-2-offload is utilized as applicable. Notably, the distributed architecture of our implementation provides flexibility in system configuration, enabling adjustments to accommodate memory and computational time constraints. Figure 9 illustrates two example configurations employed in our benchmarking experiments. **We will provide all benchmarking scripts in our codebase for reproducibility.**

- **Config 1** collocates all three workloads on each of the GPUs. Specifically, eight vLLM instances (for actors) and eight Mosec workers (for oracle RMs) are spawned to run independently on each GPU. After a batch of responses is generated (by actors) and labeled (by oracle RMs), it is sent to the learner, which runs on all eight GPUs coordinated through ZeRO strategies for policy learning. The updated policy weights are then broadcasted to all actors for *on-policy* response sampling on subsequent prompt batch. While this configuration maximizes GPU utilization, it requires substantial GPU memory to accommodate all workloads and is thus employed only for 1B scale experiments.
- **Config 2** only collocates actor and oracle workloads on half of the GPUs, reserving the remaining four GPUs exclusively for the learner. This is suited for larger-scale experiments (e.g., 2.8B or 6.9B), where additional GPU memory is allocated to the learner. However, this setup incurs idle time on half of the GPUs due to data dependency, as the learner must await new preference data, and the actor must await updated policies. An alternative is to implement *asynchronous* data collection, where minor data staleness is allowed by using θ_{t-1} to generate data for updating θ_t . Although this data would not be strictly on-policy, asynchronous training could reduce idle time and enhance GPU utilization. This approach has proven effective in large-scale RL systems (Berner et al., 2019), and we leave this optimization to future work.

Results. Benchmarking results for the latency of training a batch of 128 samples are presented in Figure 10. Overall, training with the config 2 demonstrates consistently greater efficiency than tr1, achieving up to a 2.5× reduction in latency at the 2.8B scale.

We next analyze the time costs for individual stages: generate, oracle and learn. Across all scales and configurations, ours demonstrates significantly lower *generate* time than tr1, due to distributed actors utilizing vLLM. Additionally, at the 6.9B scale, ours requires substantially less *oracle* time than tr1, as tr1 employs ZeRO-3 to prevent GPU memory overflow, thereby slowing inference. In contrast, ours config 2 allows for flexible collocation, enabling oracle RMs hosted via Mosec to operate in parallel without sharding. However, ours config 2 incurs longer *learn* time compared to tr1 due to the use of only half the available GPUs. This limitation also explains why, at the 1B scale, config 2 has higher latency than config 1 across all stages.

The *other* category accounts for time costs associated with data loading, tokenization, and communication. Here, inter-process communication is the primary cost, with tr1 showing minimal overhead as all three stages operate within the same process on identical micro-batches, avoiding weight synchronization. By contrast, ours requires considerable time to transfer updated policy weights from the learner to all actors. While NCCL

¹³<https://huggingface.co/tr1-lib/pythia-1b-deduped-tldr-rm>; <https://huggingface.co/tr1-lib/pythia-2.8b-deduped-tldr-rm>; <https://huggingface.co/tr1-lib/pythia-6.9b-deduped-tldr-rm>

1188
1189
1190
1191
1192
1193
1194
1195
1196
1197
1198
1199
1200
1201
1202
1203
1204
1205
1206
1207
1208
1209
1210
1211
1212
1213
1214
1215
1216
1217
1218
1219
1220
1221
1222
1223
1224
1225
1226
1227
1228
1229
1230
1231
1232
1233
1234
1235
1236
1237
1238
1239
1240
1241

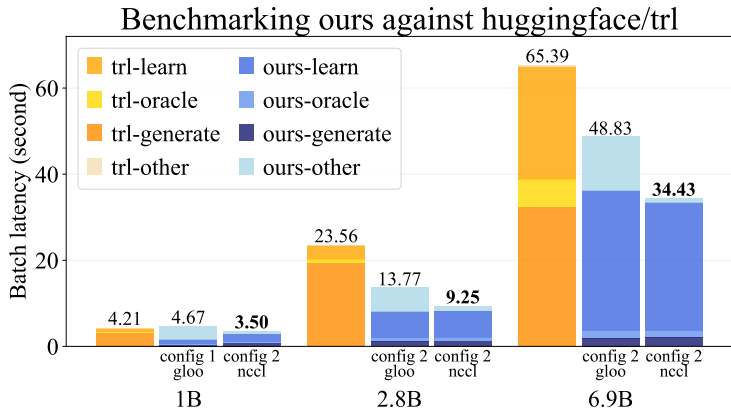


Figure 10: Averaged training latency (over 10 batches, equivalent to 1280 samples) comparing ours against huggingface/trl.

is recommended for synchronization over GLOO, it requires older vLLM packages (prior to version 0.4.3), which may lack support for newer LLM architectures. Moreover, NCCL is incompatible with config 1 due to its restriction on the learner master process establishing two separate process groups (one for DeepSpeed, the other for weight synchronization). In summary, we recommend future researchers prioritize the config 2 and employ NCCL when feasible.

G SUPPLEMENTARY MATERIALS

In this section, we include a comparison of prior works (Table 3), the prompt template we use for LLM-as-a-judge (Figure 11), and an example showing ChatGPT actively explores (Figure 7).

	Method	Exploration		Interaction			Proposal Policy	
		Active	Passive	Online	Iterative	Offline	π_θ	π_β
RL Optimizer	Christiano et al. (2017)		✓		✓	✓	✓	
	Stiennon et al. (2020)		✓		✓	✓	✓	
	Bai et al. (2022)		✓		✓	✓	✓	
	Ouyang et al. (2022)		✓		✓	✓	✓	
Direct Optimizer	Zhao et al. (2023)		✓			✓	✓	
	Rafailov et al. (2023)		✓			✓	✓	
	Azar et al. (2024)		✓			✓	✓	
	Meng et al. (2024)		✓			✓	✓	
	Xu et al. (2023)		✓		✓		✓	
	Guo et al. (2024)		✓				✓	
	Mehta et al. (2023)	✓		✓				✓
	Das et al. (2024)	✓		✓				✓
	Melo et al. (2024)	✓		✓				✓
	Dwaracherla et al. (2024)	✓		✓				✓
	Zhang et al. (2024a)	✓		✓			✓	
	Xie et al. (2024)	✓		✓			✓	
Muldrew et al. (2024)	✓		✓			✓		

Table 3: A summary of prior work. π_θ denotes the proposal policy that is continuously updated based on newly collected preference data, while π_β denotes a fixed proposal policy. Algorithms that encompass online interaction (Property 1), active exploration (Property 2), and learnable π_θ offer the best sample efficiency. Notably, only three methods (listed at the bottom of the table) satisfy these characteristics, and we include them for comparisons in our experiments.

1242
1243
1244
1245
1246
1247
1248
1249
1250
1251
1252
1253
1254
1255
1256
1257
1258
1259
1260
1261
1262
1263
1264
1265
1266
1267
1268
1269
1270
1271
1272
1273
1274
1275
1276
1277
1278
1279
1280
1281
1282
1283
1284
1285
1286
1287
1288
1289
1290
1291
1292
1293
1294
1295

LLM-as-a-Judge Prompt Template

I require a leaderboard for various large language models. I'll provide you with prompts given to these models and their corresponding outputs. Your task is to assess these responses, and select the model that produces the best output from a human perspective.

Instruction

{instruction}

Model Outputs

Here are the unordered outputs from the models. Each output is associated with a specific model, identified by a unique model identifier.

```
{  
  "model_identifier": "0",  
  "output": {response0}  
}
```

```
{  
  "model_identifier": "1",  
  "output": {response1}  
}
```

Task

Evaluate the models on the basis of the quality and relevance of their results, and select the model that generated the best result. Reply with the identifier of the best model. Our evaluation will only take into account the first character of your answer, so make sure it contains only one of the identifiers and nothing else (no quotation marks, no spaces, no new lines, ...).

Figure 11: We provide the prompt with two responses and ask GPT to choose the preferred one. We parse the first token's logits of "0" and "1" and apply the BT model to obtain the relative preference.

1296
1297
1298
1299
1300
1301
1302
1303
1304
1305
1306
1307
1308
1309
1310
1311
1312
1313
1314
1315
1316
1317
1318
1319
1320
1321
1322
1323
1324
1325
1326
1327
1328
1329
1330
1331
1332
1333
1334
1335
1336
1337
1338
1339
1340
1341
1342
1343
1344
1345
1346
1347
1348
1349

I want to use this for k8s readiness check, which requires a return value "0" if success, how to write the script?

You're giving feedback on a new version of ChatGPT.

Which response do you prefer? Responses may take a moment to load.

Response 1

To create a script for a Kubernetes readiness check using `curl`, where you return a `0` status on success (typically when the HTTP status code is `200`), you can combine `curl` with a conditional check on the HTTP status code. If the status is `200`, the script will exit with `0` (indicating success); otherwise, it will return a non-zero value (indicating failure).

Here's an example of how you can write this script:

```
bash
#!/bin/bash

# Send a POST request and get the HTTP status code
STATUS=$(curl -X POST -H "Content-Type: application/octet-st

# Check if the status code is 200
if [ "$STATUS" -eq 200 ]; then
    exit 0 # Readiness check successful
else
    exit 1 # Readiness check failed
fi
```

Explanation:

- `curl` sends the request and captures the HTTP status code in the `STATUS` variable.
- The `if` statement checks if the status code is `200`.
 - If the status code is `200`, the script exits with `0`, indicating success (readiness).
 - If the status is anything other than `200`, the script exits with `1`, indicating failure.

You can modify the binary string or URL as necessary for your specific readiness check.

I prefer this response

Response 2

Memory updated

For a Kubernetes readiness check, you need to return `0` if the `curl` command succeeds (e.g., status code `200`), and a non-zero value if it fails.

Here's a simple bash script that achieves this:

```
bash
#!/bin/bash

URL="<your-endpoint>"
STATUS_CODE=$(curl -X POST -H "Content-Type: application/oct

if [ "$STATUS_CODE" -eq 200 ]; then
    exit 0 # success
else
    exit 1 # failure
fi
```

Breakdown:

- `curl ... -w "%{http_code}"`: Captures the HTTP status code from the `curl` request.
- The `if` condition checks if the status code is `200` (indicating success).
- `exit 0`: Indicates a successful readiness check.
- `exit 1`: Indicates failure, so Kubernetes will consider the pod not ready.

You can adjust the script depending on the specific status code(s) that you consider successful.

I prefer this response

Figure 12: ChatGPT system asks for users' preference feedback to strategically explore better answers. In this case, algorithms should be designed around the objective of *minimizing cumulative regret* (i.e., the E&E setting), because the quality of both responses generated by the system affects user experience.